



UNIVERSITY OF STOCKHOLM

INSTITUTE OF PHYSICS

A STUDY OF THE INTERPRETATIONS OF CHARM
PARTICLE DECAYS INTO THREE CHARGED
PARTICLES IN NA16

T. MOA

A STUDY OF THE INTERPRETATIONS OF CHARM PARTICLE DECAYS INTO THREE CHARGED
PARTICLES IN NA16

T. Moa

Institute of Physics, University of Stockholm
Vanadisvägen 9, S-113 46 Stockholm

ABSTRACT

The variation of the kinematic fit probability as a function of the mass of the decaying particle is studied for all hypotheses tried for the three prong charged decays in the NA16 LEBC-EHS experiment.

The choice of interpretation we make for the various observed decays is based on the fits obtained by the kinematic fitting program. The procedure used in making the choice can be outlined as follows (criteria I):

- Choose hypothesis with highest number of constraints.
- Choose hypothesis with smallest number of seen neutrals (π^0 or η).
- Choose D before F or Λ_c .

There is no hierarchy in these choices, so we cannot distinguish between e.g. a D-hypothesis with two π^0 's and an F with one π^0 .

This method will of course introduce biases, as we are likely to get an excess of events in the D-channels without π^0 's, e.g. the $D^+ \rightarrow K^-\pi^+\pi^+$ channel which is used in calculating the total D^+ cross section.

In an attempt to test the reliability of the choices made, we have studied the variation of the kinematic fit probability as a function of the mass of the decaying particle for any given hypothesis (criteria II).

In this study we have used 24 3-prong decays and 1 1-prong decay giving 3-C fits, i.e. having all tracks hybridized. These events have been run through the kinematics fitting program a number of times, using for each run slightly modified mass values for D^+ , F and Λ_c . The masses were varied in steps of 20 MeV/c² in most cases, 10 MeV/c² in some, and covered a mass range of ± 60 MeV/c² from the nominal mass values. The nominal values used here are the values normally used by the kinematics program, and they are 1868.3 MeV/c², 2040 MeV/c² and 2273 MeV/c² for the D^+ , F and Λ_c , respectively. All the 3C-hypotheses of every event were uniquely identified using the hypothesis number and the labels of the seen neutrals attached to it, and the fit probability was recorded for all mass values. The fit probability was then plotted versus the mass, and a gaussian was fitted to each set of points, to serve as a "guideline for the eye". These plots are all presented in figs. 1 through 25. They are presented separately for every event, and also for different number of seen neutrals attached to the hypotheses.

Since the number of data points is very low in many cases, great care should be taken when trying to draw any conclusions from the shapes of the curves, as the fits can be quite unreliable. Nevertheless, there are three general features of these curves that can be pointed out:

- The probability function of any given hypothesis peaks at the invariant mass calculated from the measured quantities. This is clearly shown in fig. 26, where we have plotted the mass versus the mean of the fitted gaussian, and also the ratio between these numbers. The mean value of that ratio is found to be $1.002 \pm .003$.
- The width ($=\sigma$) of the fitted gaussian is equal to the error in the measured invariant mass of the hypothesis. From fig. 27b we find the mean value of the ratio between these two numbers to be $1.00 \pm .03$.
- The height of the peak is determined by the goodness of the transverse momentum conservation. That explains why, for many of the plots, the heights do not vary very much within one event, since the momenta are not altered by the change of particle masses for the tracks. When adding neutral particles seen in the spectrometer, however, the net momentum vary with the particle added, thus the variation that we see can be understood.

From these features it is possible to draw the conclusion that, given a set of measured tracks, the "best" hypothesis can be defined as the one having the highest probability. In the case where the measured tracks vary from one hypothesis to another, however, e.g. when different π^0 's are used, the heights and widths of the curves are no longer the same, and therefore the definition of the "best" hypothesis is not so straight forward.

Here follows a short description of each decay in the light of these plots, and a comparison with the standard interpretation. The decays are referenced by the roll- and frame-numbers. Please note that there is no distinction of the charges, i.e. $\bar{\Lambda}_C$ is denoted Λ_C in the following.

069-3364 This is clearly a D, and it serves as a good example of the decisive

power of the kinematics when all tracks are well measured.

072-5635 Also this decay is a clear D.

075-7361 This is the only one-prong decay in the study, and it was included because it has always been a good candidate for an F.

081-0380 Although slightly high in mass, this is also considered to be a good F-candidate, especially as there is only one OC-solution for this decay, and that one is also an F.

084-8766 A very poor momentum measurement ($\delta p/p > 10\%$) on one of the tracks from this decay makes a decision almost impossible, but using the information in the plots one would be tempted to call this a Λ_c . Due to the bad measurement, however, this decay has been moved into the "zoo" category, i.e. we know from the topology that it is charm, but we cannot identify it.

085-1753 Following our standard procedure of choosing D before F or Λ_c , this decay has been called a D. Looking at the plots, however, would give a much higher weight to the F or Λ_c fits with no neutral. The charge is negative, so the Λ_c (or $\bar{\Lambda}_c$ as it would be) is not likely.

087-6800 This decay suffers from a multitude of (spurious) π^0 combinations in addition to a γ converting in the chamber. The γ is used by the kinematics as a K^0 or a Λ in the plots including the " ν^0 " in the header so they can be discarded. In the remaining plots there are several possible solutions present, and apart from the D with one π^0 that the standard procedure would pick we can mention at least one good F with one π^0 , and three or more D-hypotheses with two π^0 's.

102-4843 Due to the present uncertainty in the determination of the true mass value for the F, the D-hypothesis must be considered the best choice for this decay.

103-7889 The D-hypothesis is the only possible.

113-8206 Looking at the probability plots, this event is likely to be an F, but according to the standard selection criteria we would favour the

D-hypothesis with no π^0 before anything with one π^0 .

116-1135 The standard procedure would pick the D with one π^0 for this decay, but the probability distributions give one good F with one π^0 , and a handful of possible D's with two π^0 's.

120-6828 This decay has been called an F/Λ_c ambiguity, and given the uncertainty of the F and Λ_c masses, we cannot make a firm decision.

127-5724 As can be seen from the large width of the distributions, this event has a very badly measured track, and has therefore been moved into the "zoo".

144-5401 Here is another case where the standard selection procedure possibly introduces biases. The hypothesis chosen by it is a D with one π^0 , having 0.1 % probability at the correct D mass. This is in fact the only D hypothesis with one π^0 that has a non-zero probability at the D. However, as is clearly seen from the plots, the choice is likely not to be correct, but an overwhelming multitude of π^0 's makes any firm choice impossible.

148-0207 This is in many ways a doubtful decay. The lifetime is large, 53×10^{-13} s for the D-hypothesis, and it is outside the charm box, i.e. the transverse distance $|\Delta y| > 0.06$ cm. The fit probabilities are also rather low, indicating that the transverse momenta just barely can be made to balance.

149-1190 Since all plots look equally bad, we cannot do other than to call this a $D/F/\Lambda_c$ ambiguity. This was also the original assignment.

149-2024 The charge of this decay is negative, and hence we can disregard the Λ_c hypothesis as being not very likely. Thus, this is a good D.

152-6910 Here is a clear D hypothesis.

158-6037 The original selection procedure has not been able to identify this decay, and we cannot do much more from these plots, so it is called $D/F/\Lambda_c$ ambiguous.

162-8219 This decay, having only F-hypotheses, is considered a good

F-candidate.

173-0217 The V^0 in this event is likely to be a γ and this reduces the number of possibilities considerably. However, there are still too many to make a choice so it has been called a D/F ambiguity.

178-0649 Selecting the D before the Λ_c could well be wrong in this case. The Λ_c has $p_T = 0.94$ GeV/c and $x_F = 0.94$ and lifetime = 1.4×10^{-13} s, but we cannot discard the D.

178-0653 Also this decay is dubious. This has been called a D with one π^0 , but many other possibilities clearly exist.

179-6924 The standard procedure would select a very good D in this case, but clearly there are other possibilities, e.g. a D with one π^0 as well as a few F's with two π^0 's.

181-3256 A rather poor momentum measurement together with a large number of π^0 's gives a variety of possible solutions for this decay. From these plots we cannot, however, see any reason to discard the choice made by the standard procedure.

A summary of the criteria I choices vs. the criteria II can be found in table 1. The "zoo"-decays and the dubious 148-0207 are not included in the table. As can be seen from this table, 5 out of 22 decays gets a somewhat different interpretation. For the D-decays, the situation is summarized in table 2. From a total of 9 decays previously believed to be $D^+ \rightarrow K^+ \pi^+ \pi^+$, 2 have a possibility for being F or Λ_c . This gives a crude estimate of an upper limit for the background of falsely identified $K\pi\pi$ decays.

The conclusion we can draw from this investigation is that in events with well measured tracks and a small number of π^0 's in the gamma detectors, the information we have is sufficient to establish the nature of the decaying particles. This is true at least as long as we believe in the general selection of 3C fits before 0C solutions.

Acknowledgements

The data on charmproduction in the CERN experiment NA16 (Amsterdam - Brussels - CERN - Madrid - Mons - Nijmegen - Oxford - Padova - Paris - Rome - Rutherford laboratory - Serpukhov - Stockholm - Trieste - Vienna collaboration) are the basis for this work. In particular the work of Marie-Claude Touboul and Peter Wright to produce the final Data Summary Tape for NA16 is gratefully acknowledged. Thanks are also due to Sven Olof Holmgren, Sigward Nilsson and Erik Johansson for discussions and moral support.

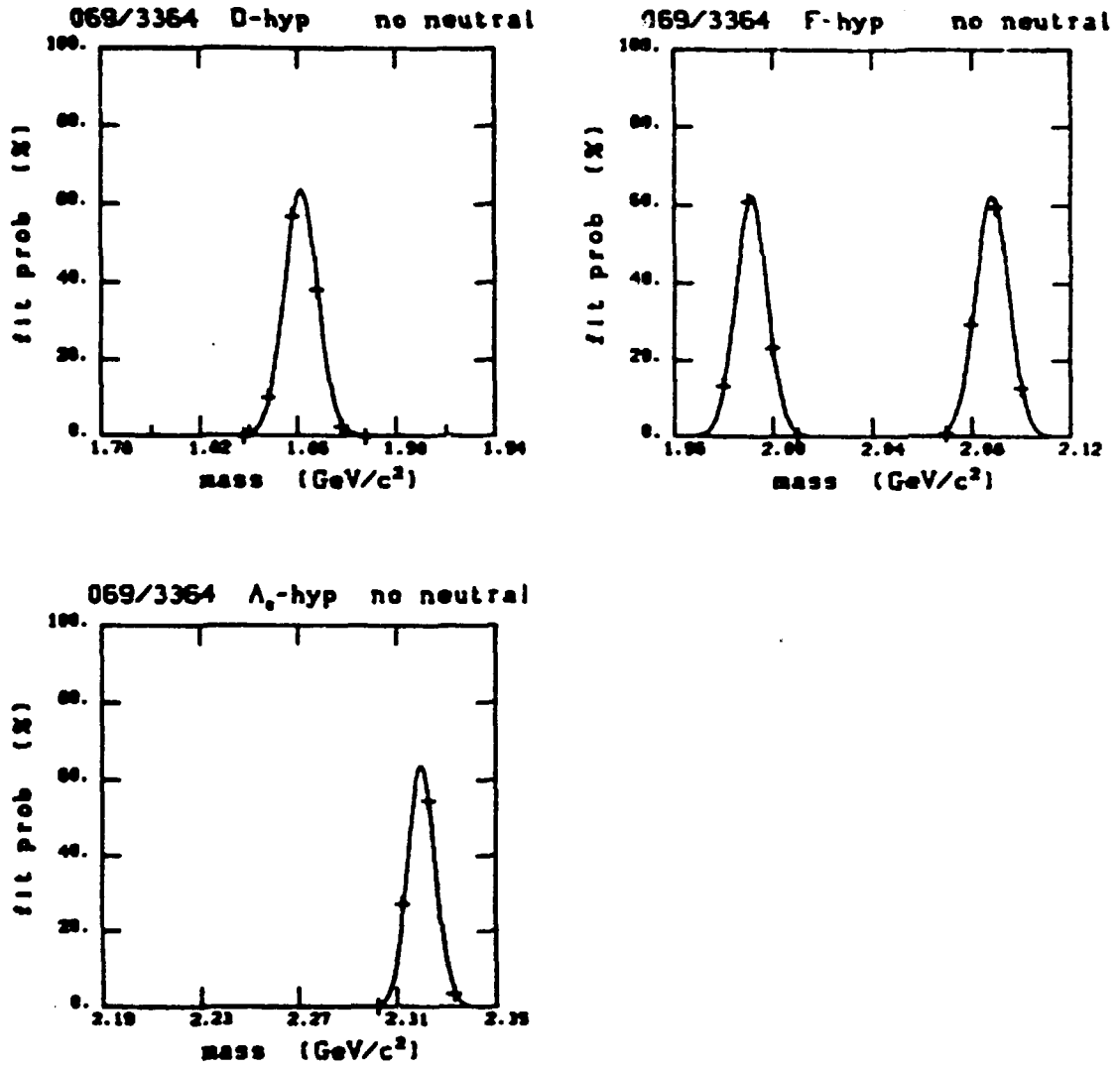


Fig. 1 (a-c). Fit probability vs. mass, frame 069-3364.

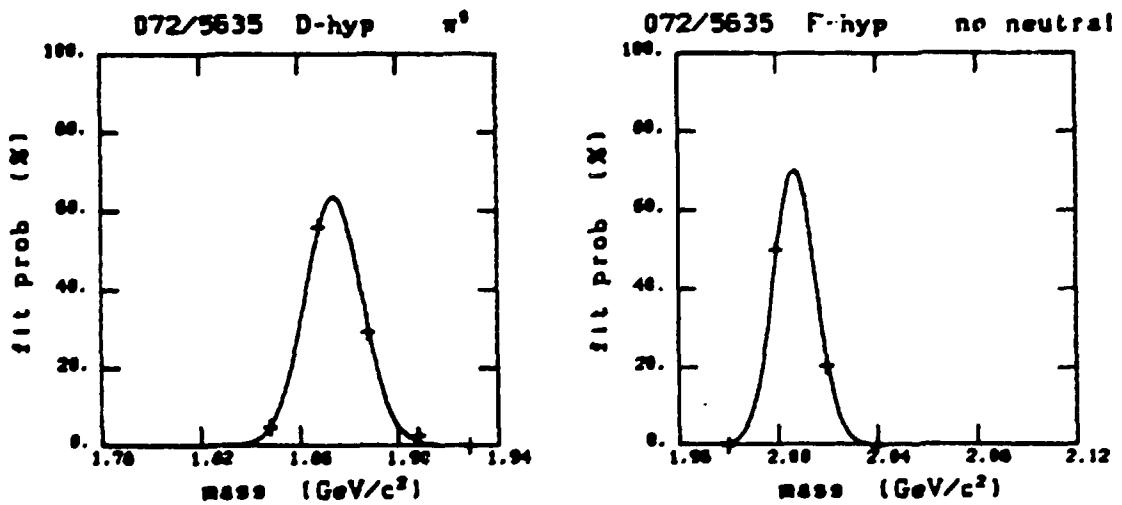


Fig. 2 (a-b). Fit probability vs. mass, frame 072-5635. (Continued).

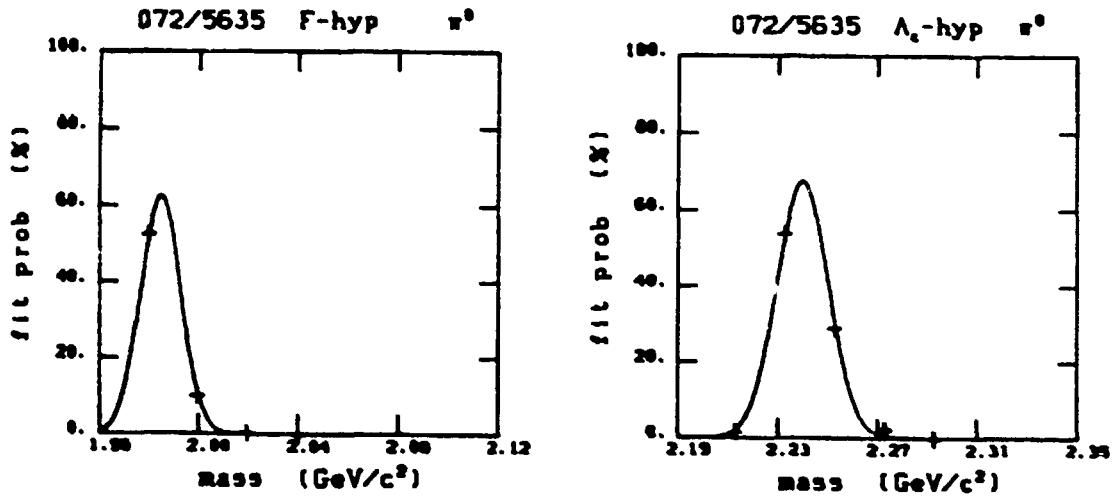


Fig. 2 (c-d). Continued.

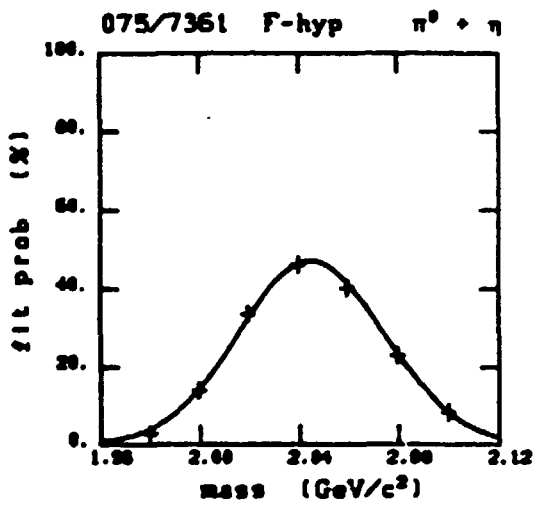


Fig. 3. Fit probability vs. mass, frame 075-7361.

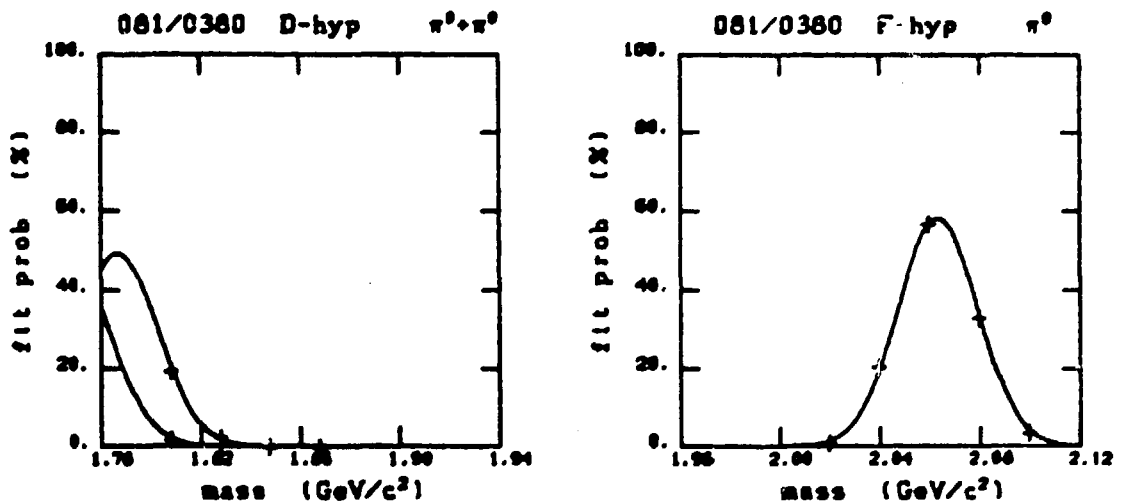


Fig. 4 (a-b). Fit probability vs. mass, frame 081-0380.

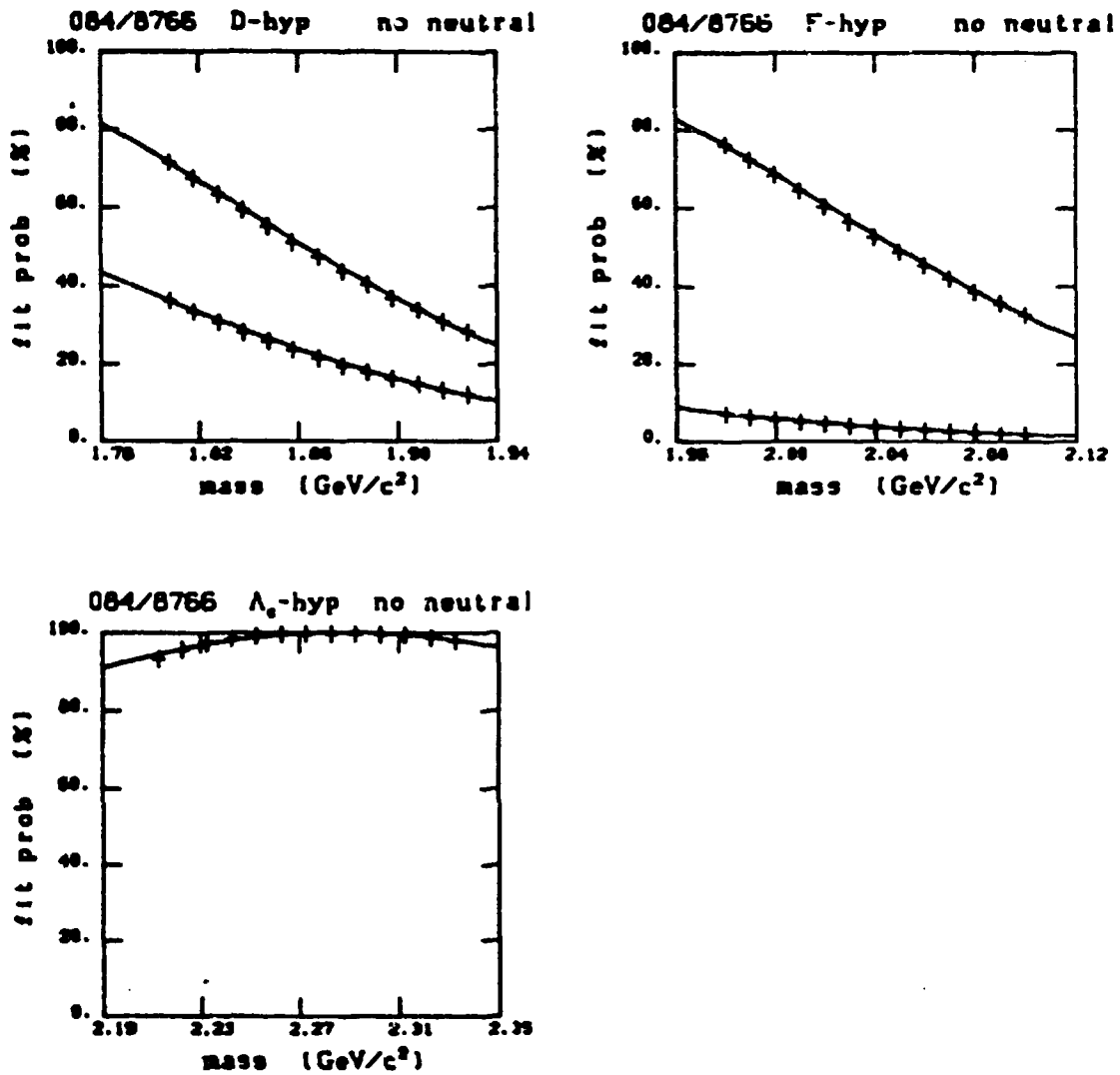


Fig. 5 (a-c). Fit probability vs. mass, frame 084-8766.

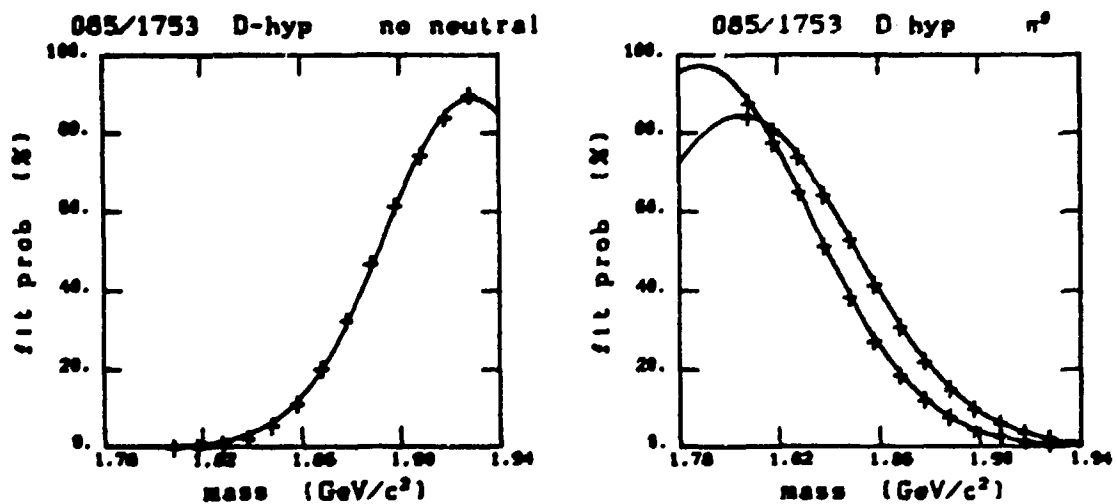


Fig. 6 (a-b). Fit probability vs. mass, frame 085-1753. (Continued).

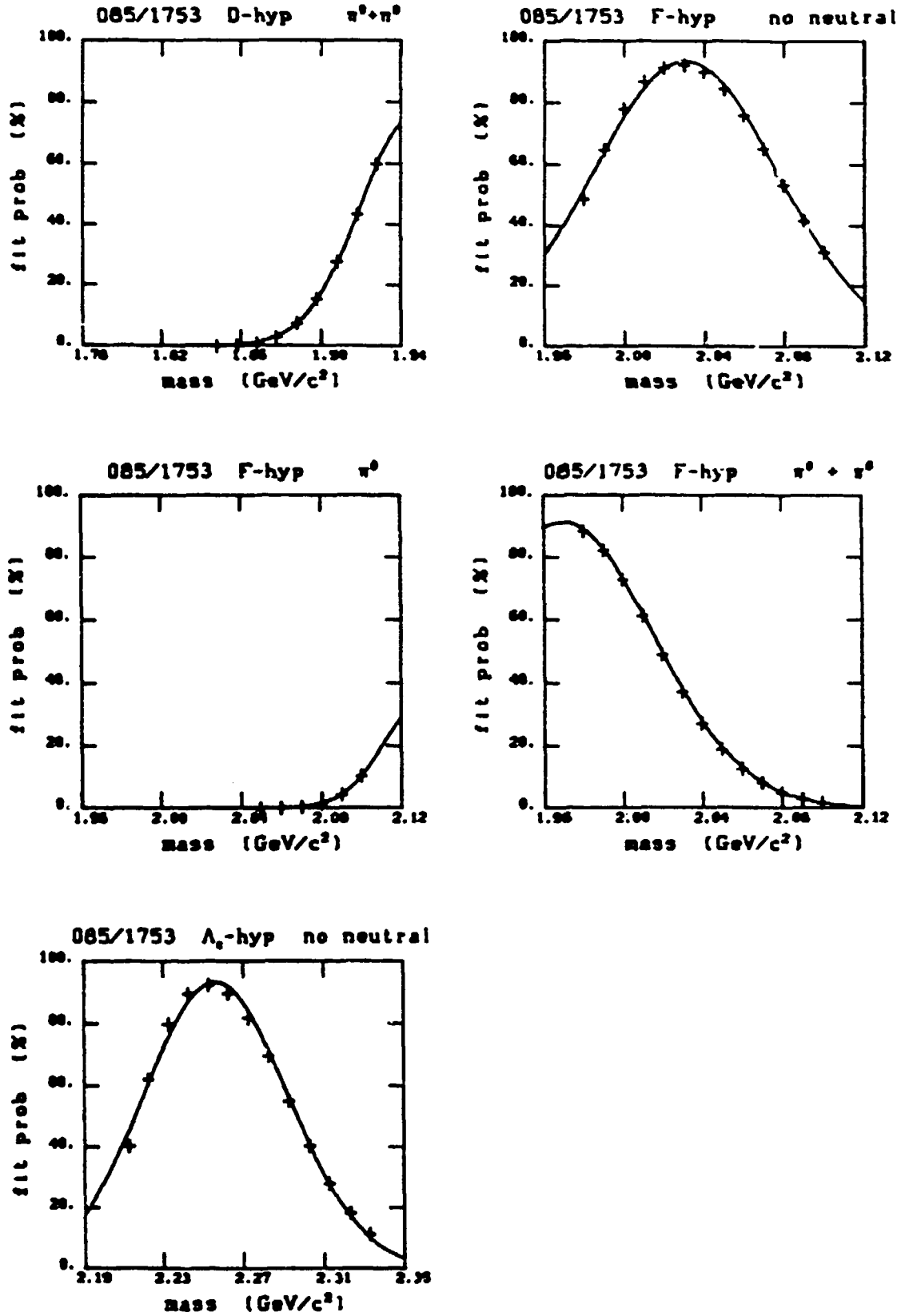


Fig. 6 (c-g). Continued.

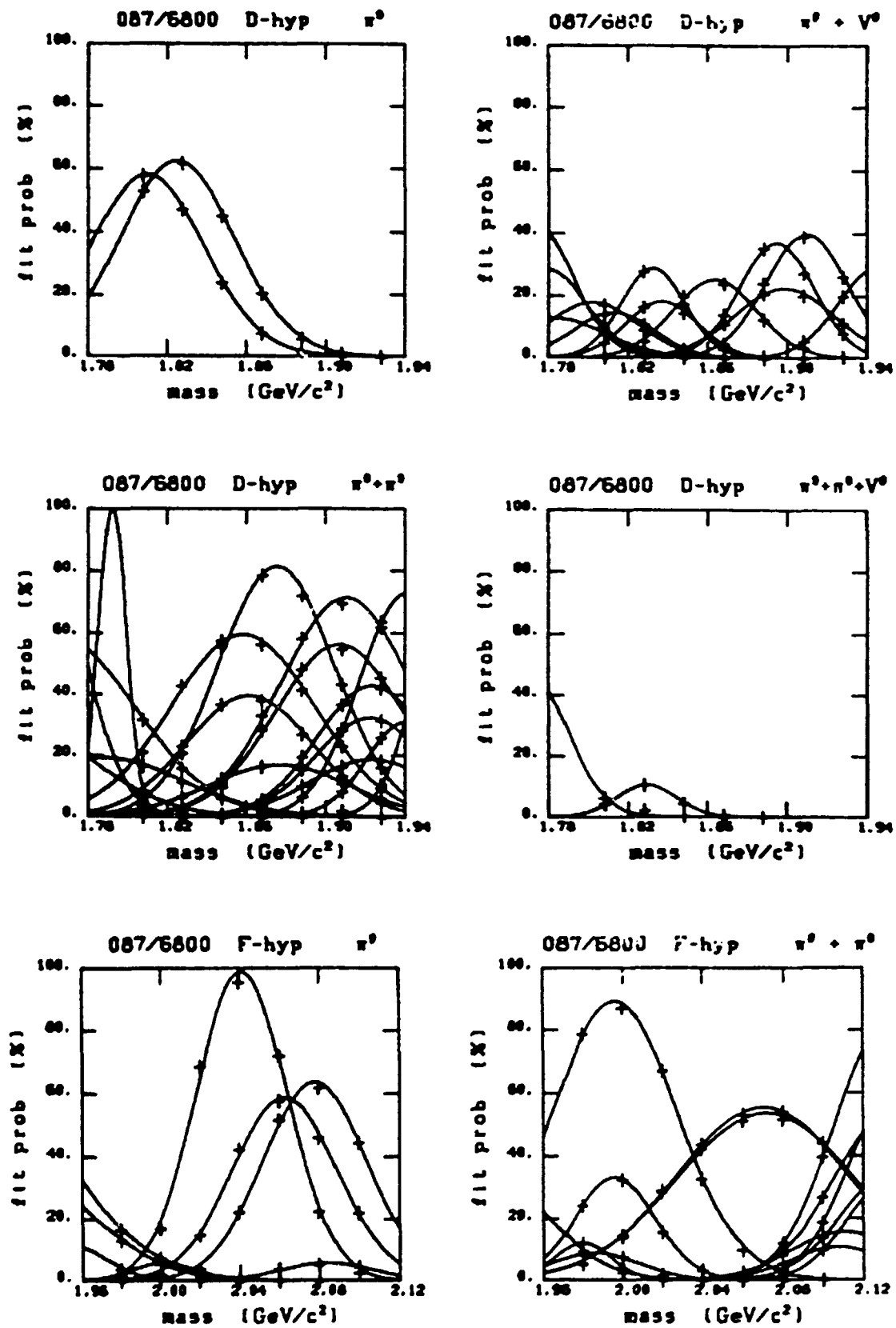


Fig. 7 (a-f). Fit probability vs. mass, frame 087-6800. (Continued).

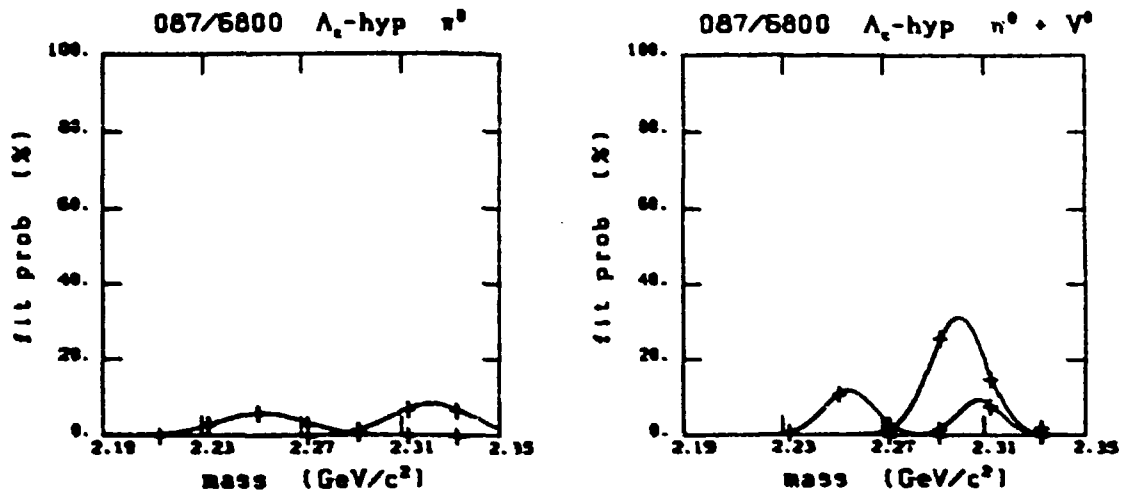


Fig. 7 (g-h). Continued.

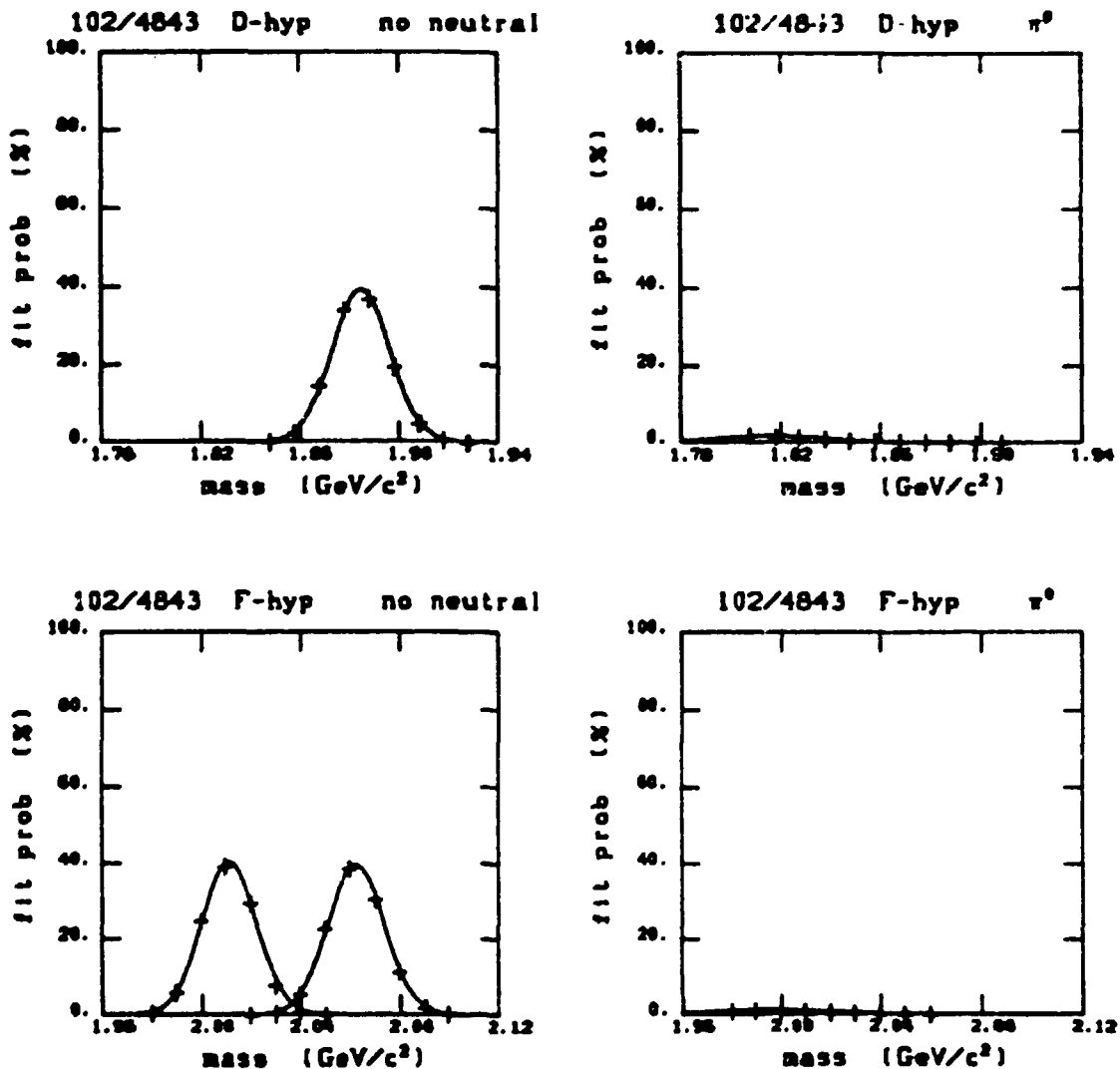


Fig. 8 (a-d). Fit probability vs. mass, frame 102-4843. (Continued.)

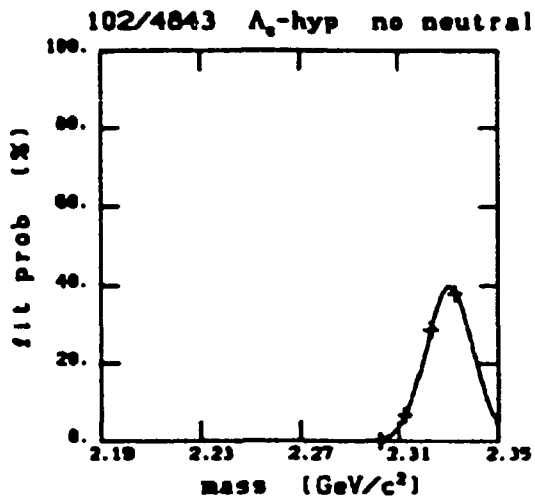


Fig. 8 (e). Continued.

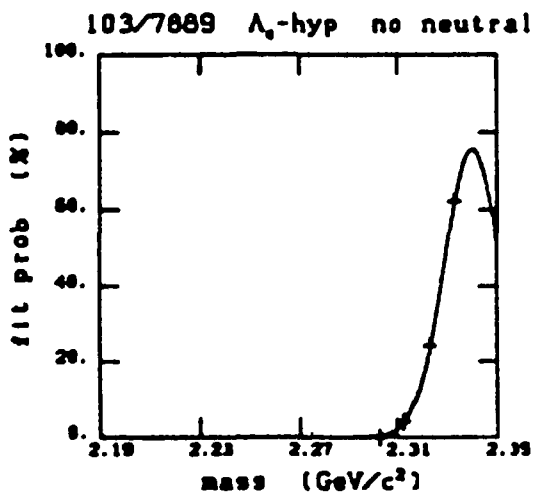
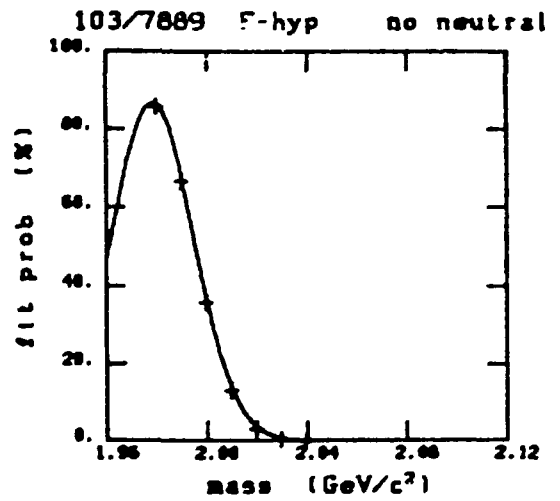
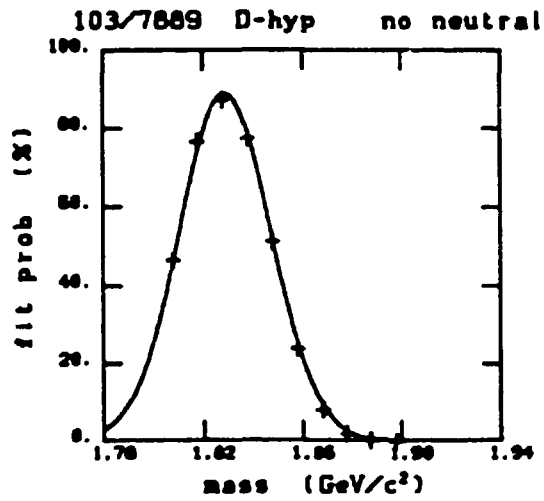


Fig. 9 (a-c). Fit probability vs. mass, frame 103-7889.

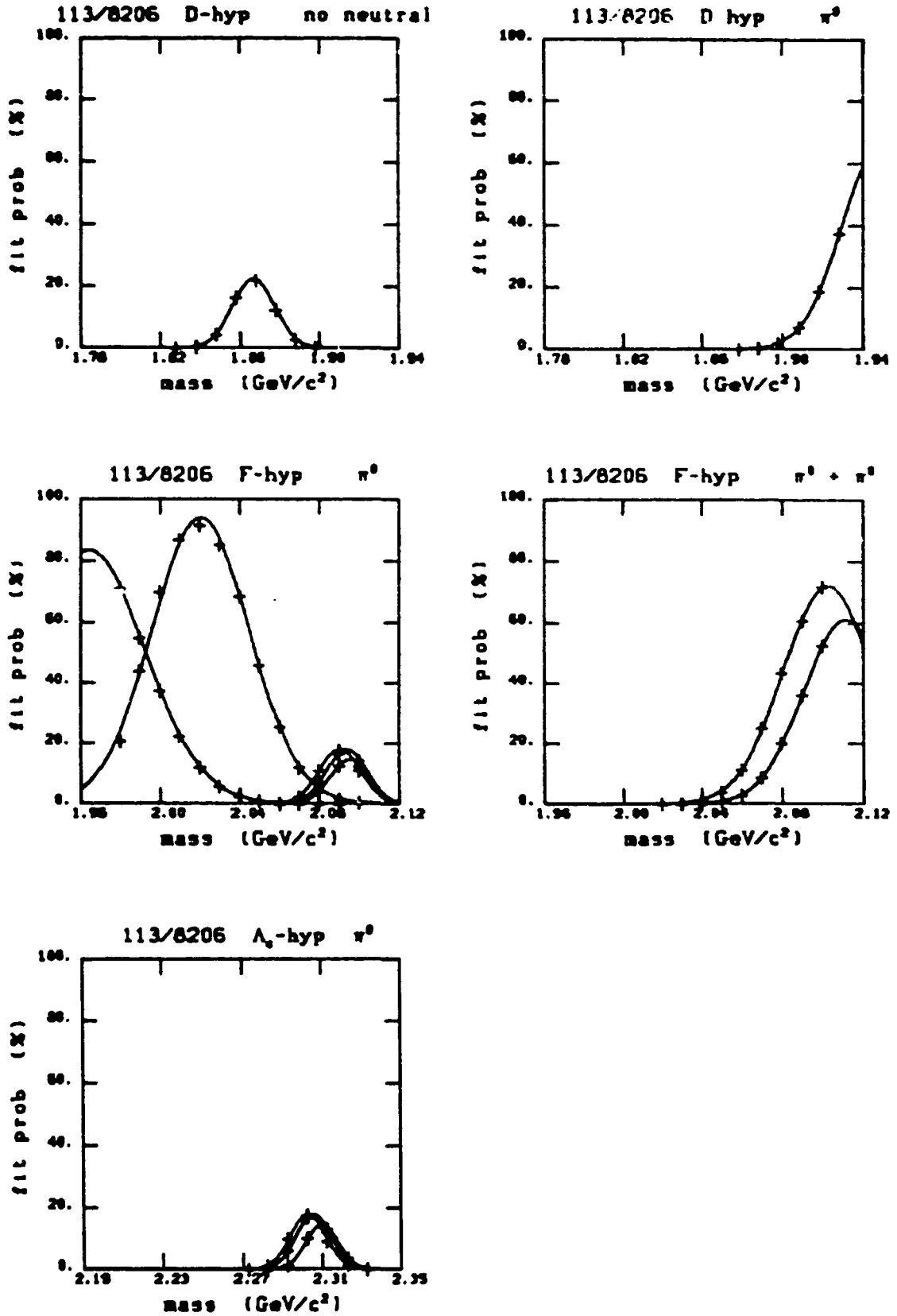


Fig. 10 (a-e). Fit probability vs. mass, frame 113-8206.

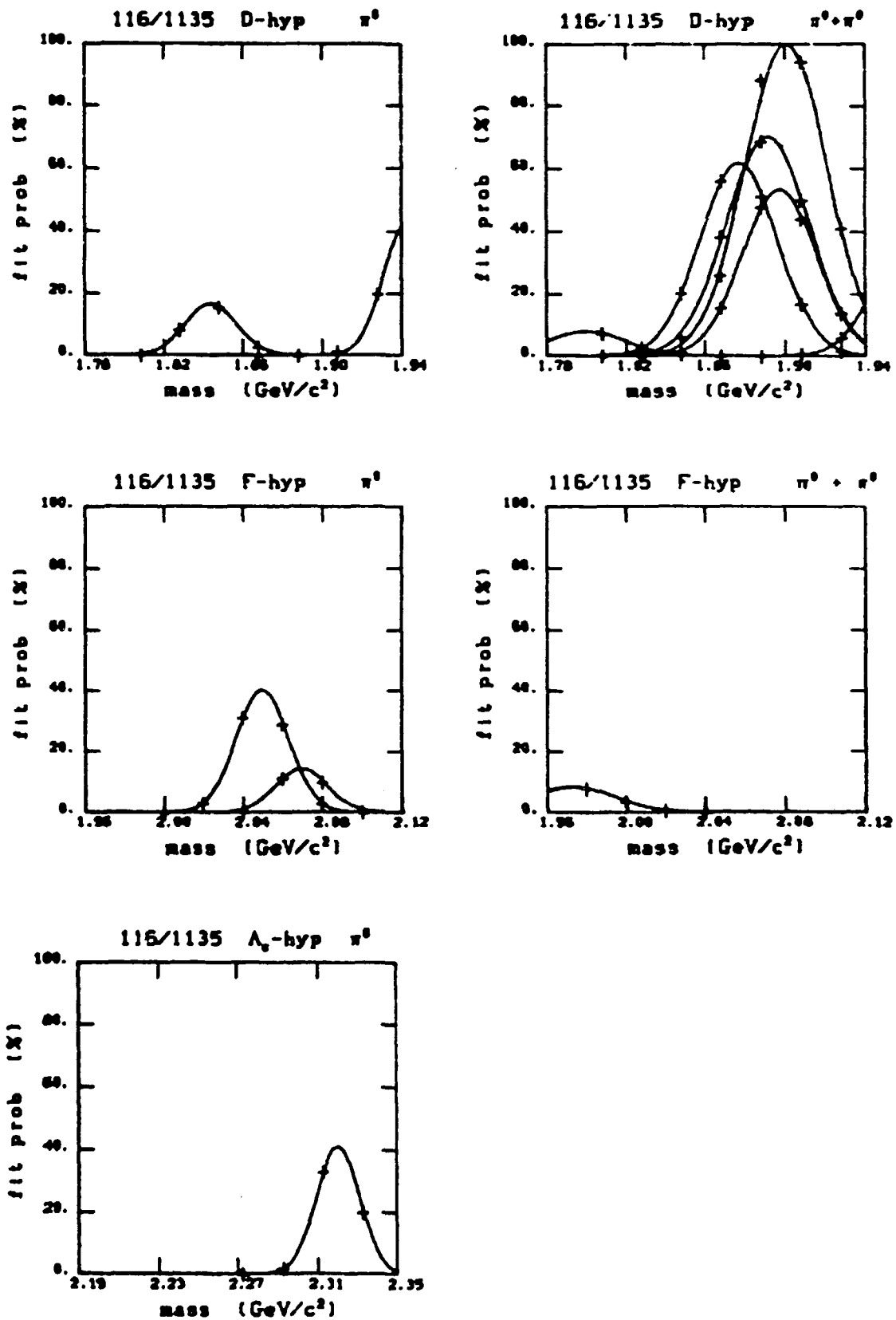


Fig. 11 (a-e). Fit probability vs. mass, frame 116-1135.

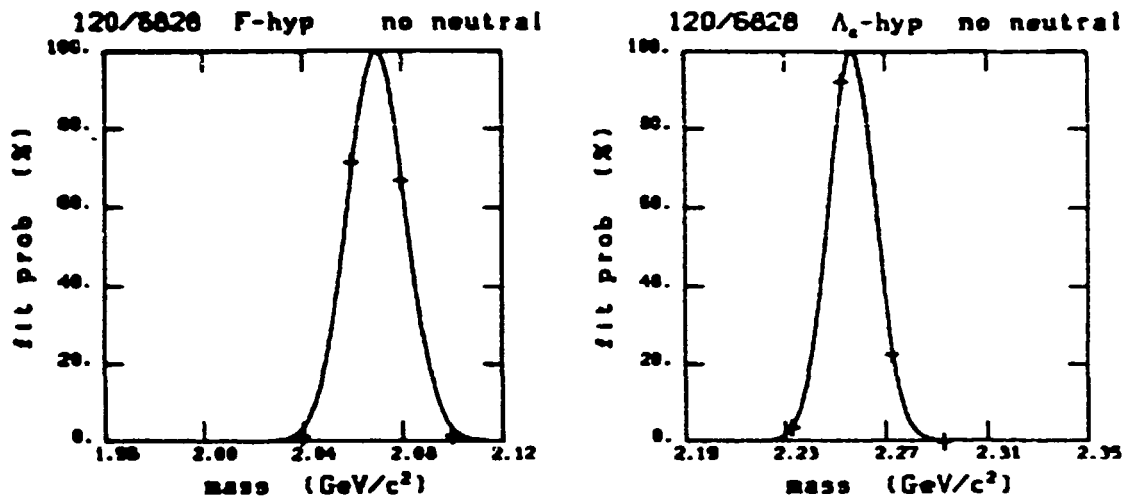


Fig. 12 (a-b). Fit probability vs. mass, frame 120-6828.

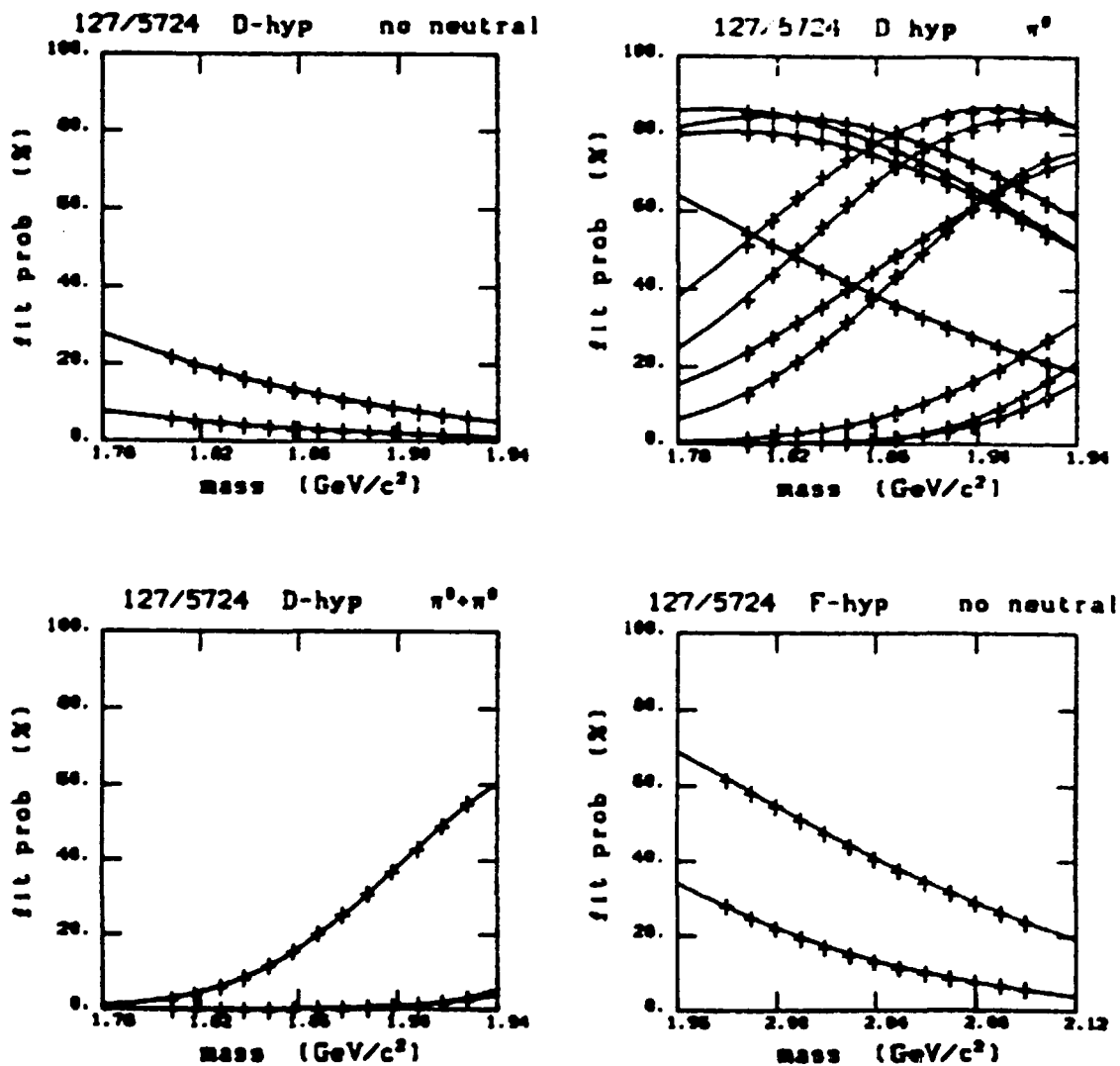


Fig. 13 (a-d). Fit probability vs. mass, frame 127-5724. (Continued.)

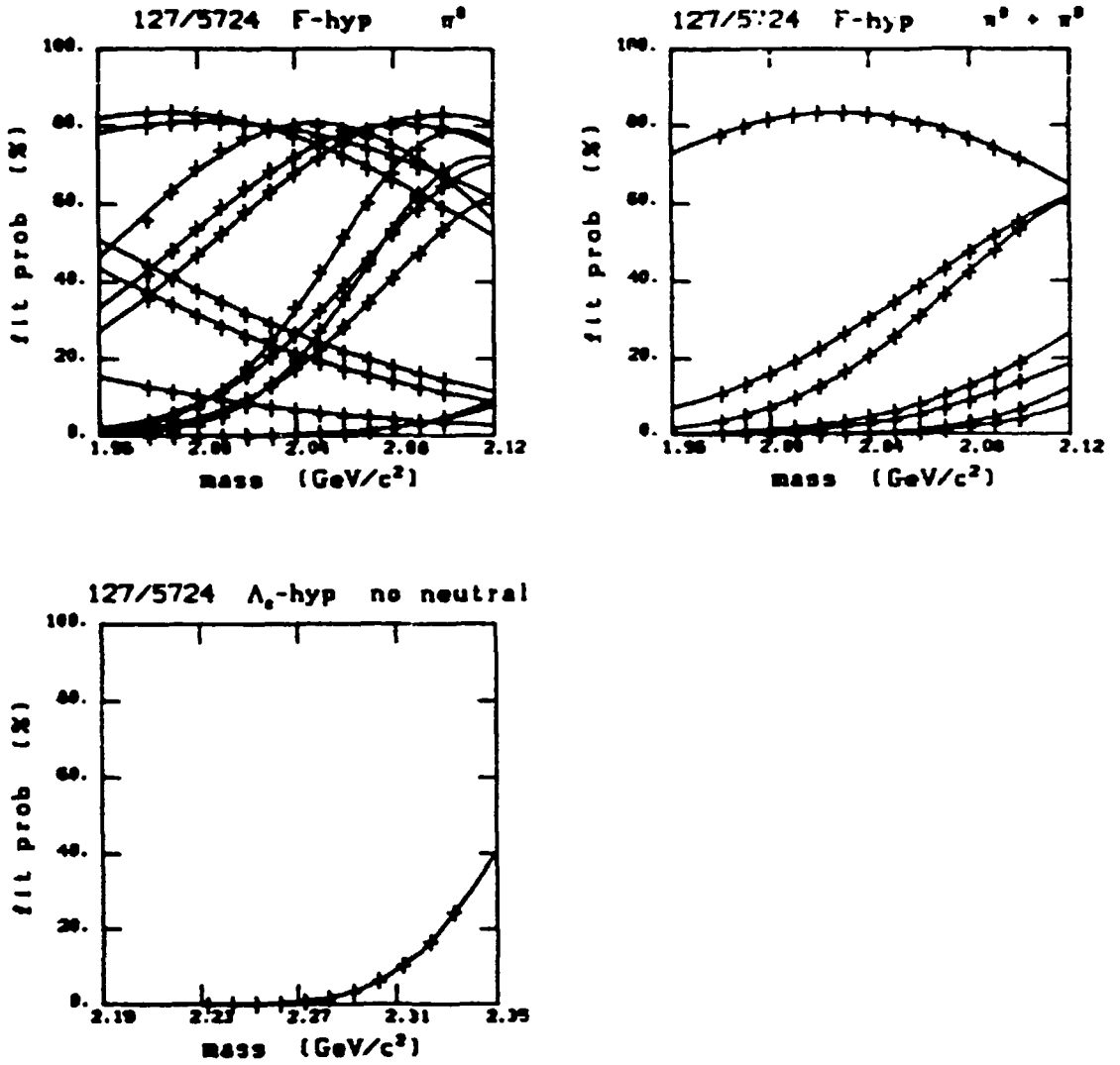


Fig. 13 (e-g). Continued.

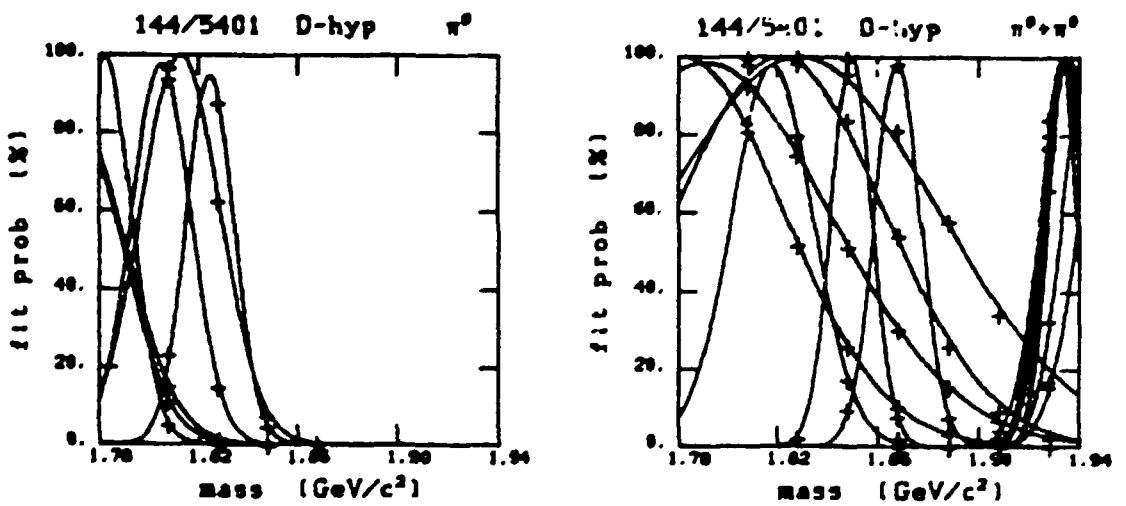


Fig. 14 (a-b). Fit probability vs. mass, frame 144-5401. (Continued.)

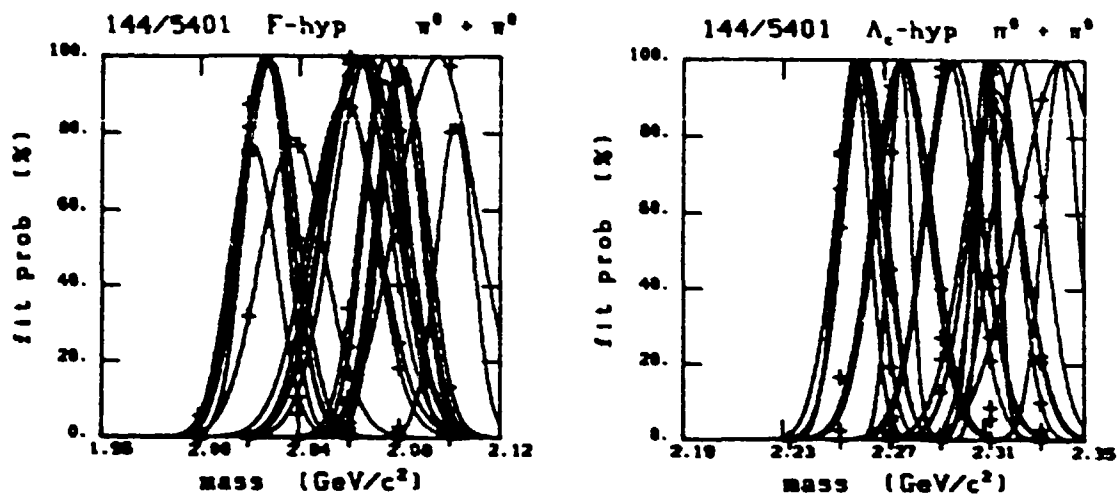


Fig. 14 (c-d). Continued.

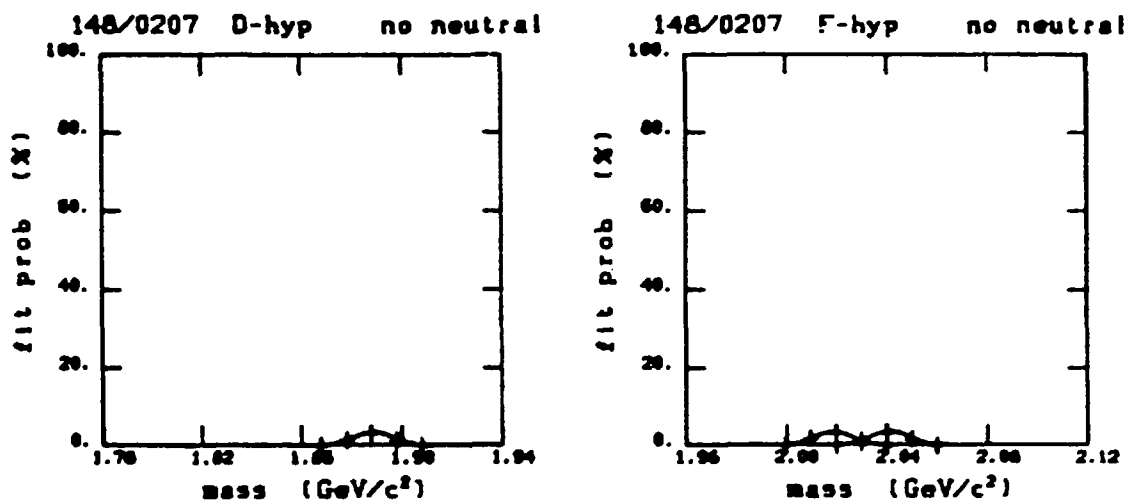


Fig. 15 (a-b). Fit probability vs. mass, frame 148-0207.

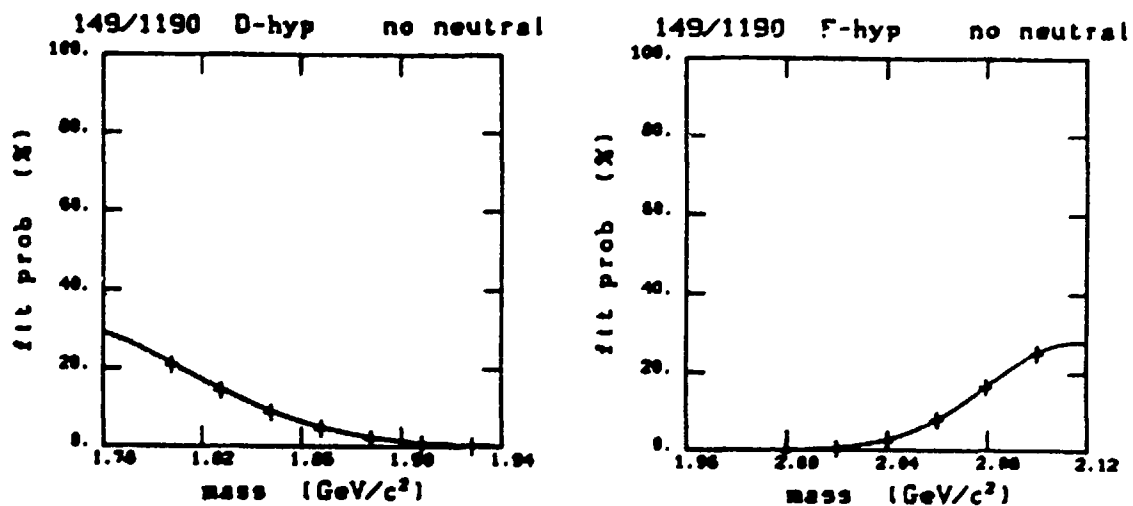


Fig. 16 (a-b). Fit probability vs. mass, frame 149-1190. (Continued.)

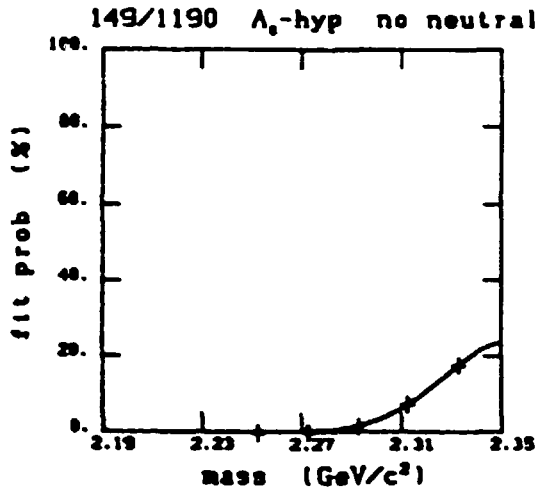


Fig. 16 (c). Continued.

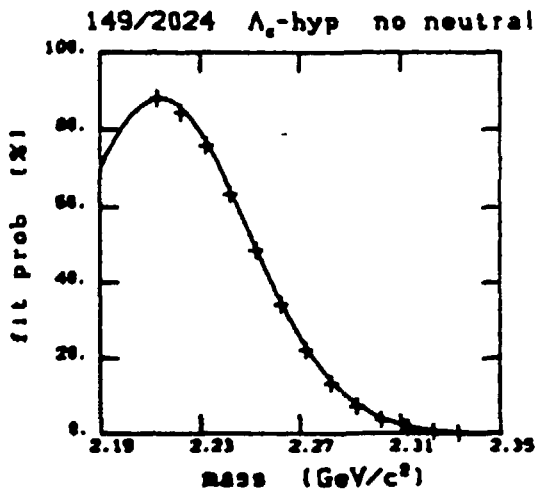
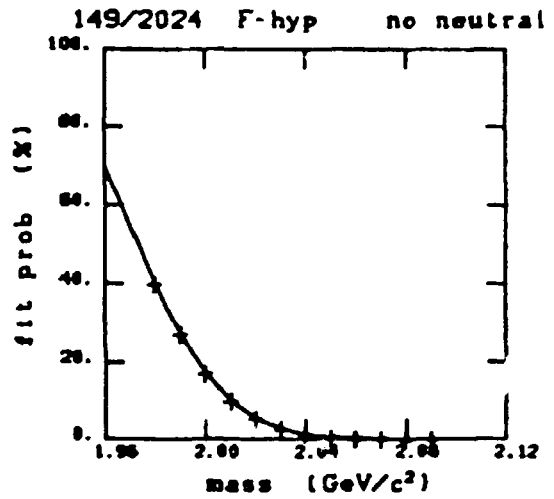
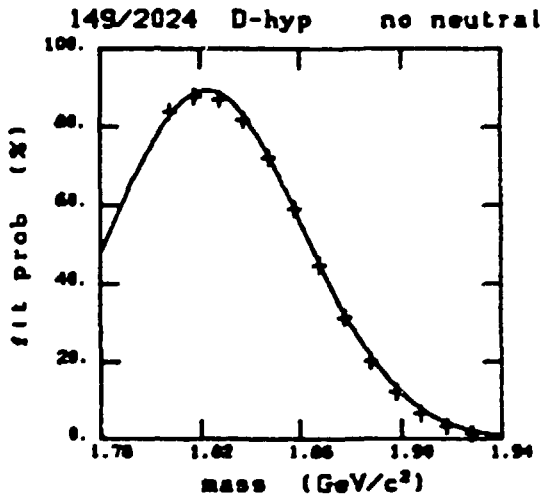


Fig. 17 (a-c). Fit probability vs. mass, frame 149-2024.

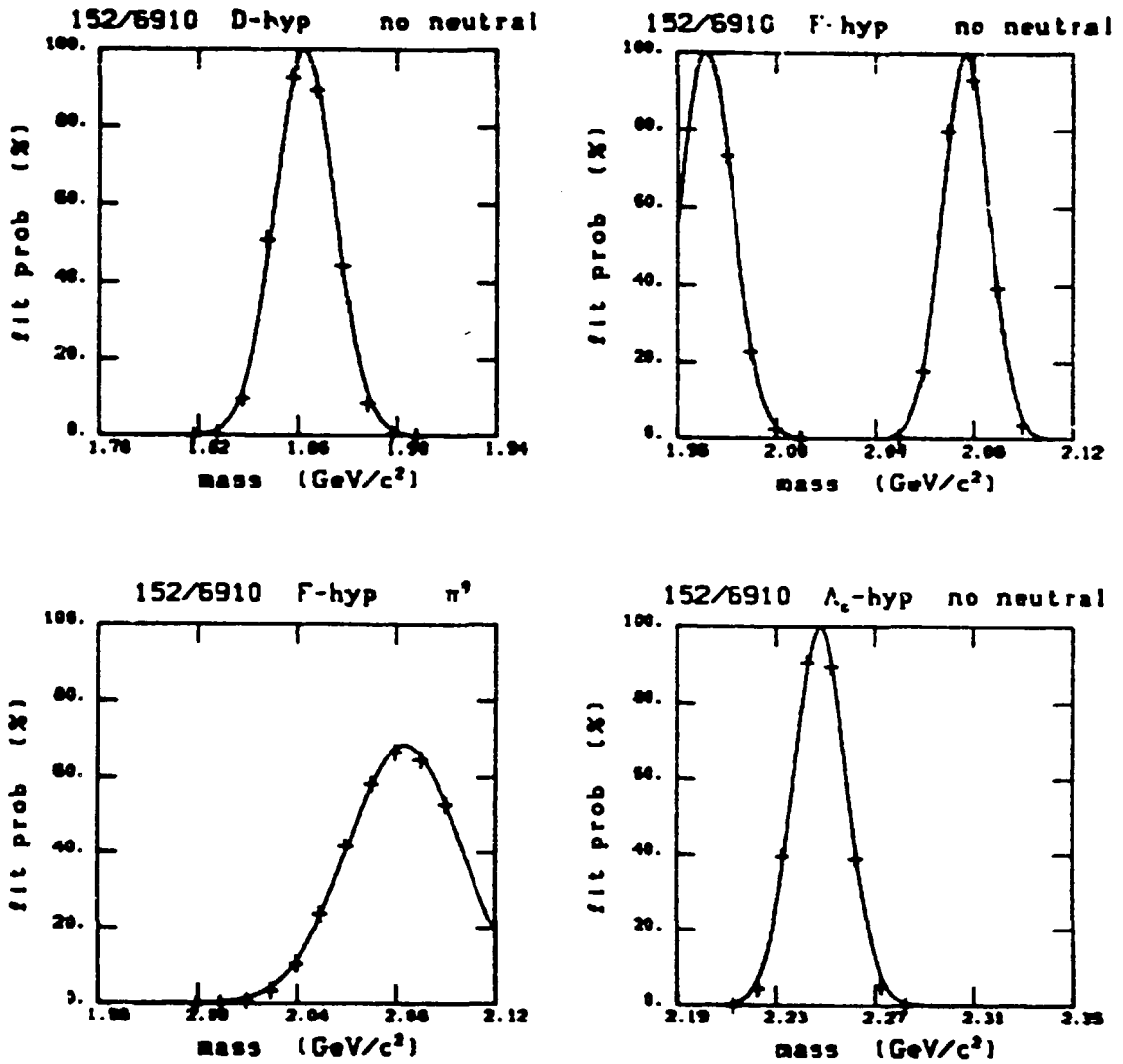


Fig. 18 (a-d). Fit probability vs. mass, frame 152-6910.

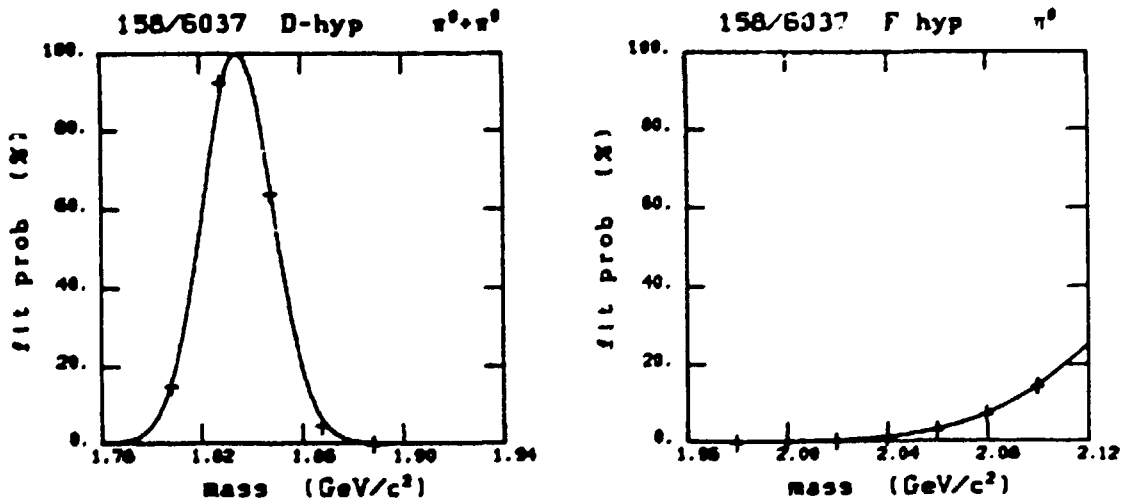


Fig. 19 (a-b). Fit probability vs. mass, frame 158-6037. (Continued.)

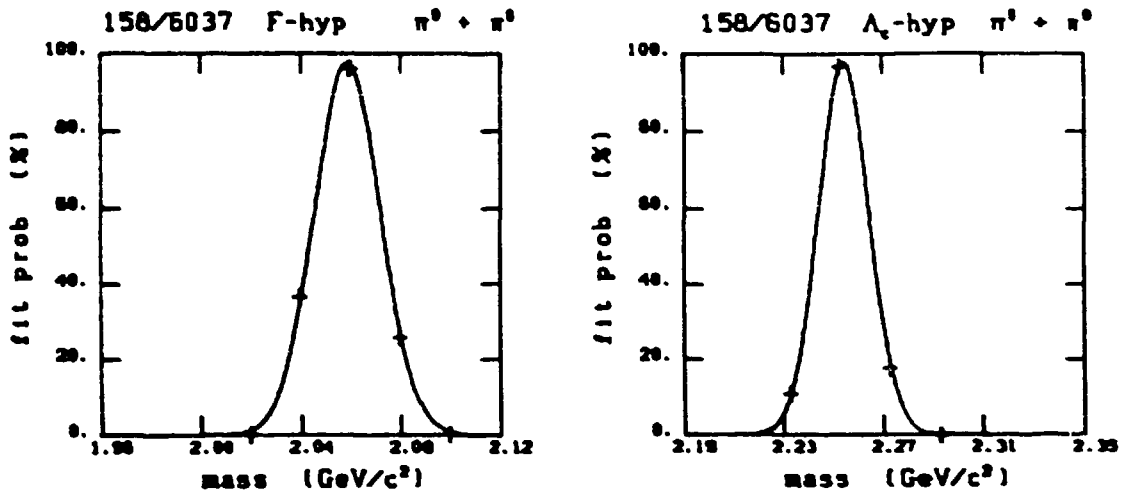


Fig. 19 (c-d). Continued.

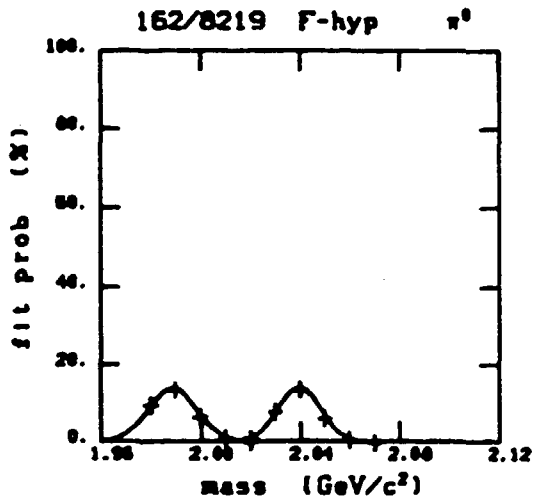


Fig. 20. Fit probability vs. mass, frame 162-8219.

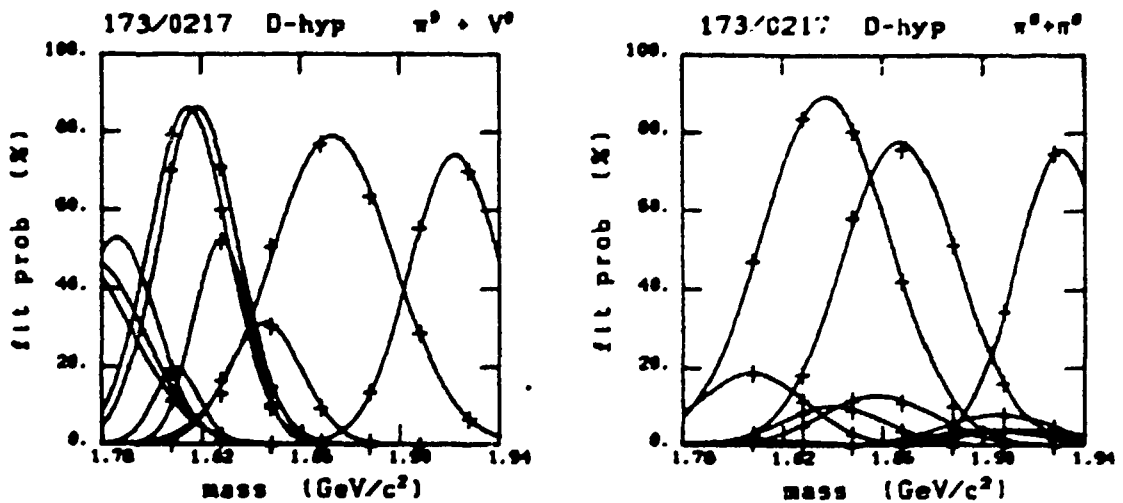


Fig. 21 (a-b). Fit probability vs. mass, frame 173-0217. (Continued.)

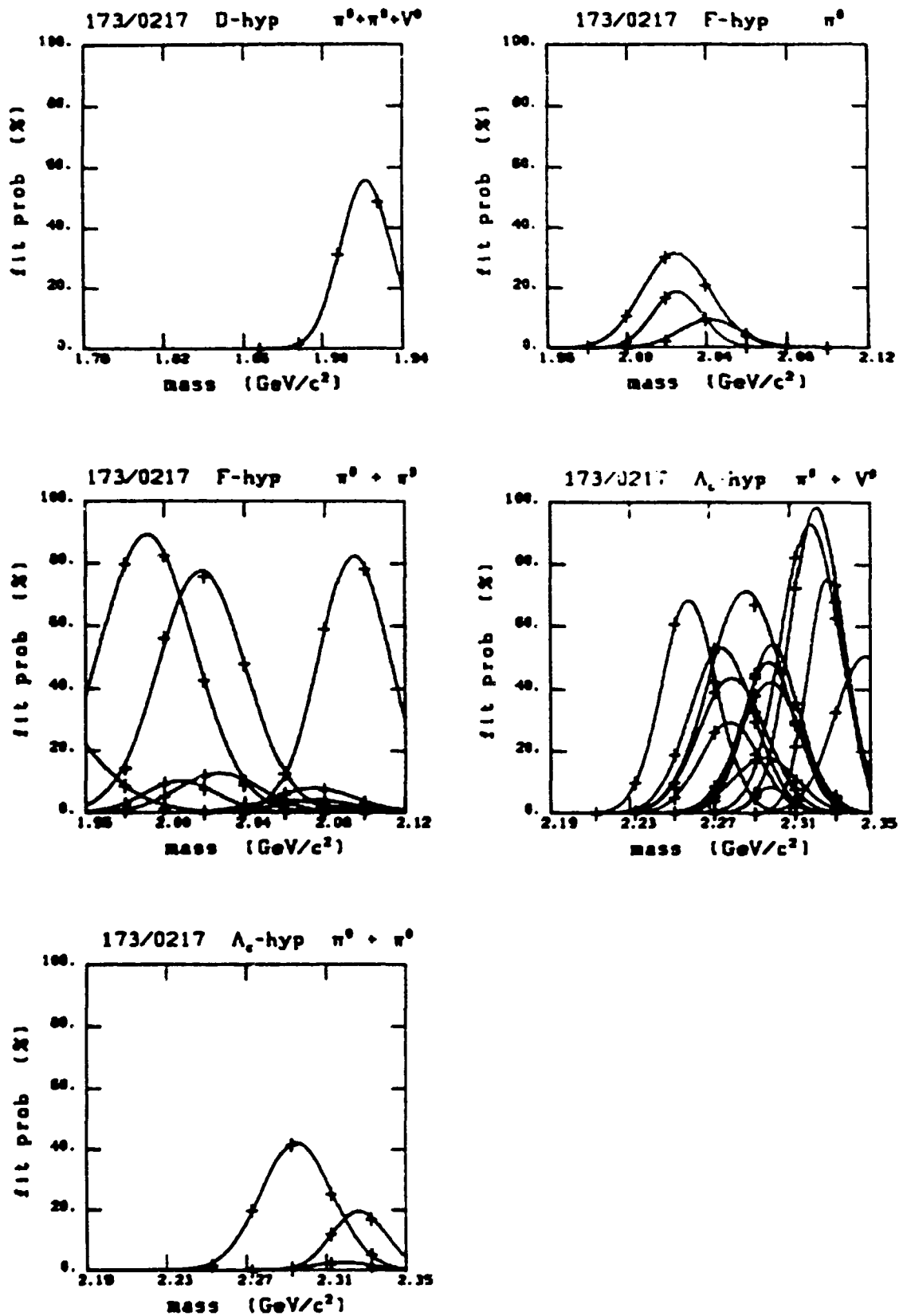


Fig. 21 (c-g). Continued.

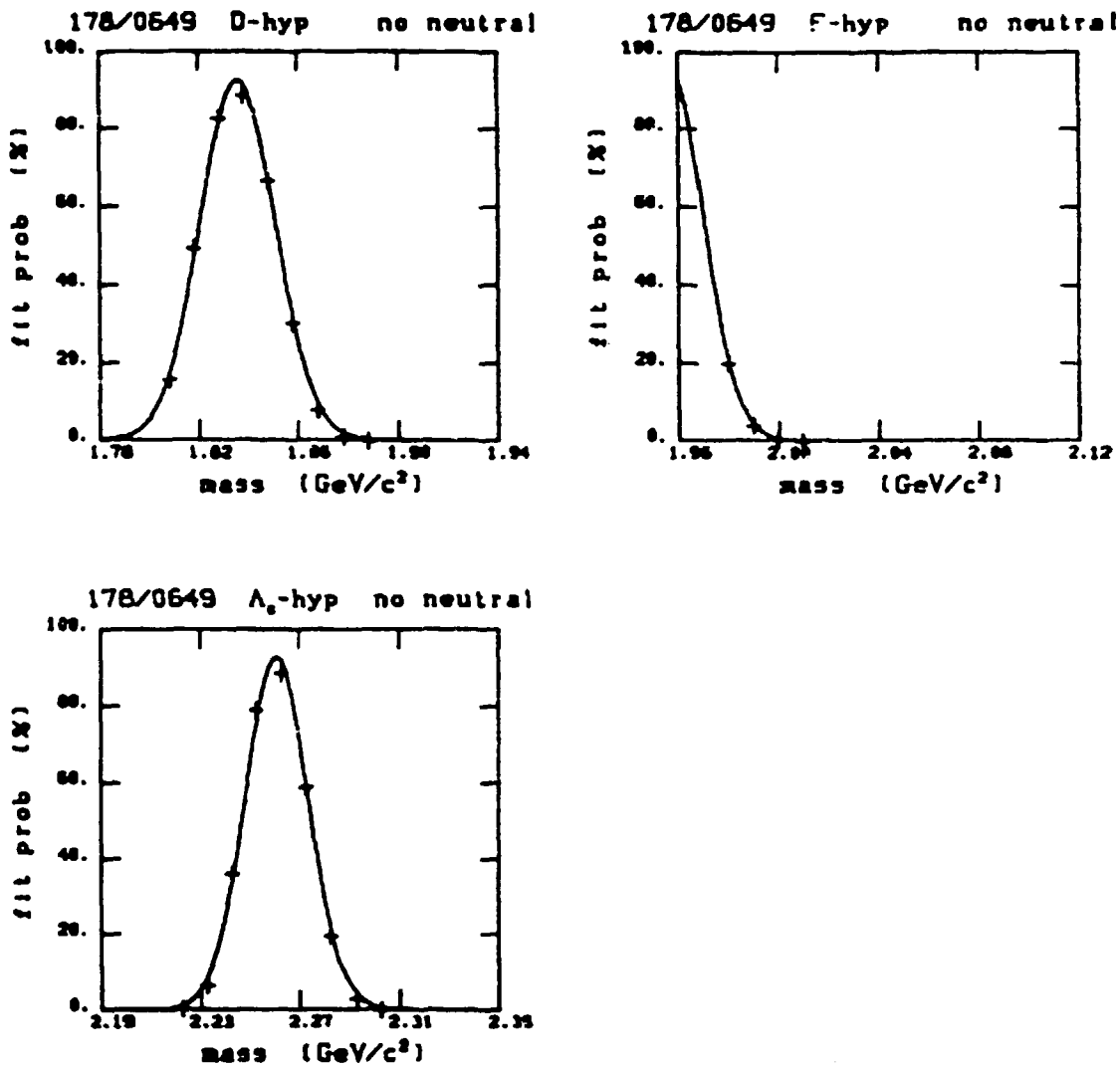


Fig. 22 (a-c). Fit probability vs. mass, frame 178-0649.

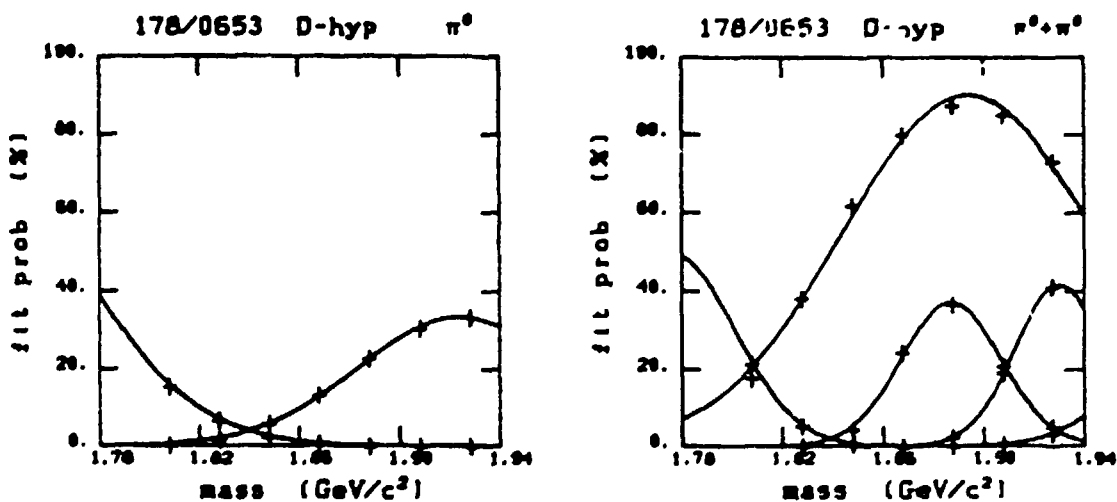


Fig. 23 (a-b). Fit probability vs. mass, frame 178-0653. (Continued.)

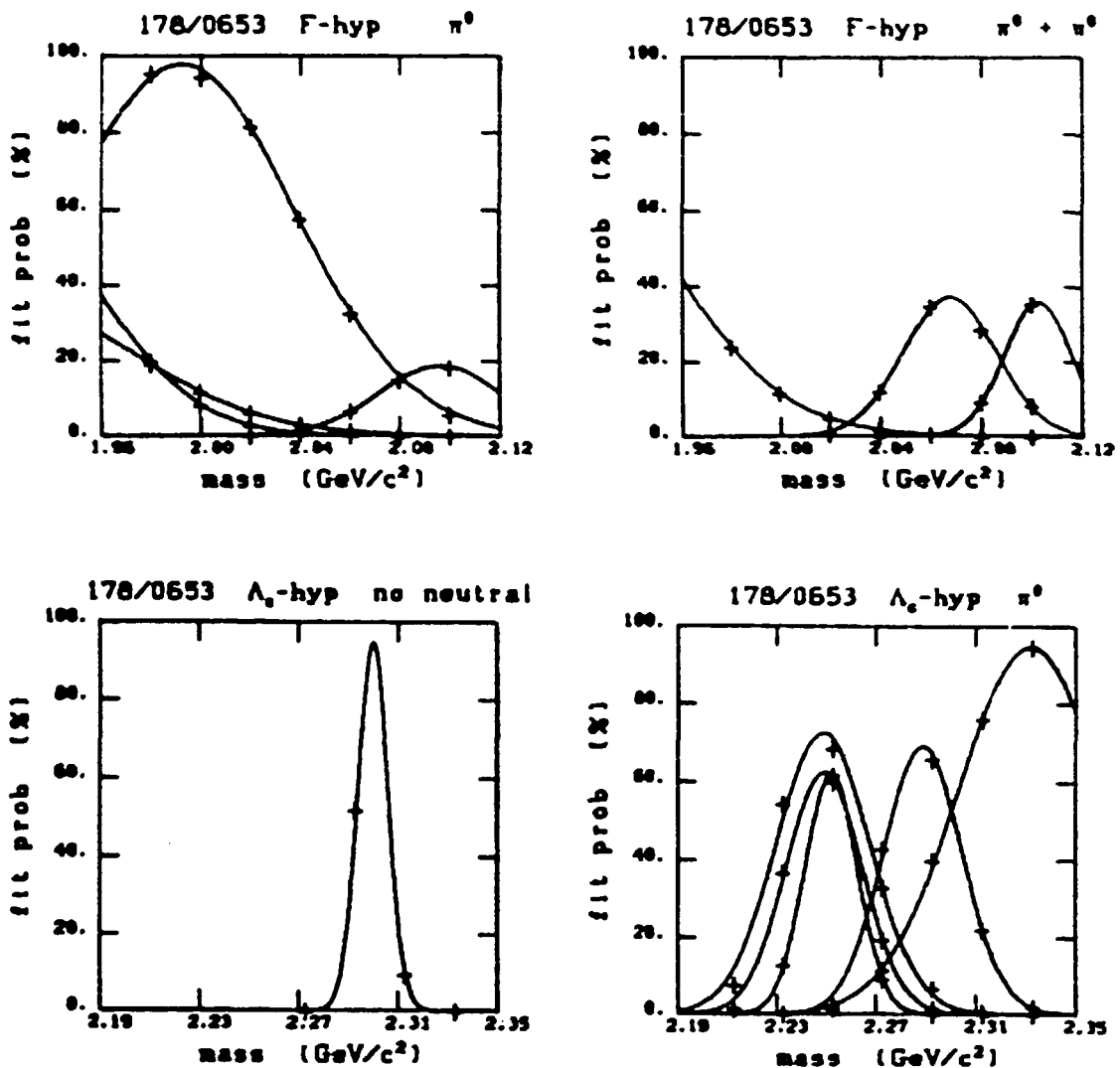


Fig. 23 (c-f). Continued.

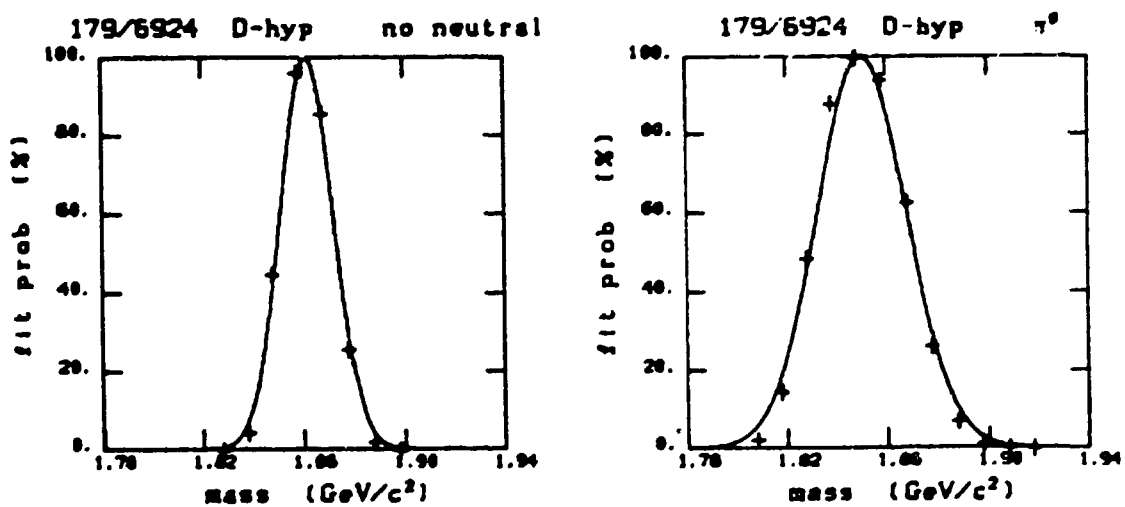


Fig. 24 (a-b). Fit probability vs. mass, frame 179-6924. (Continued.)

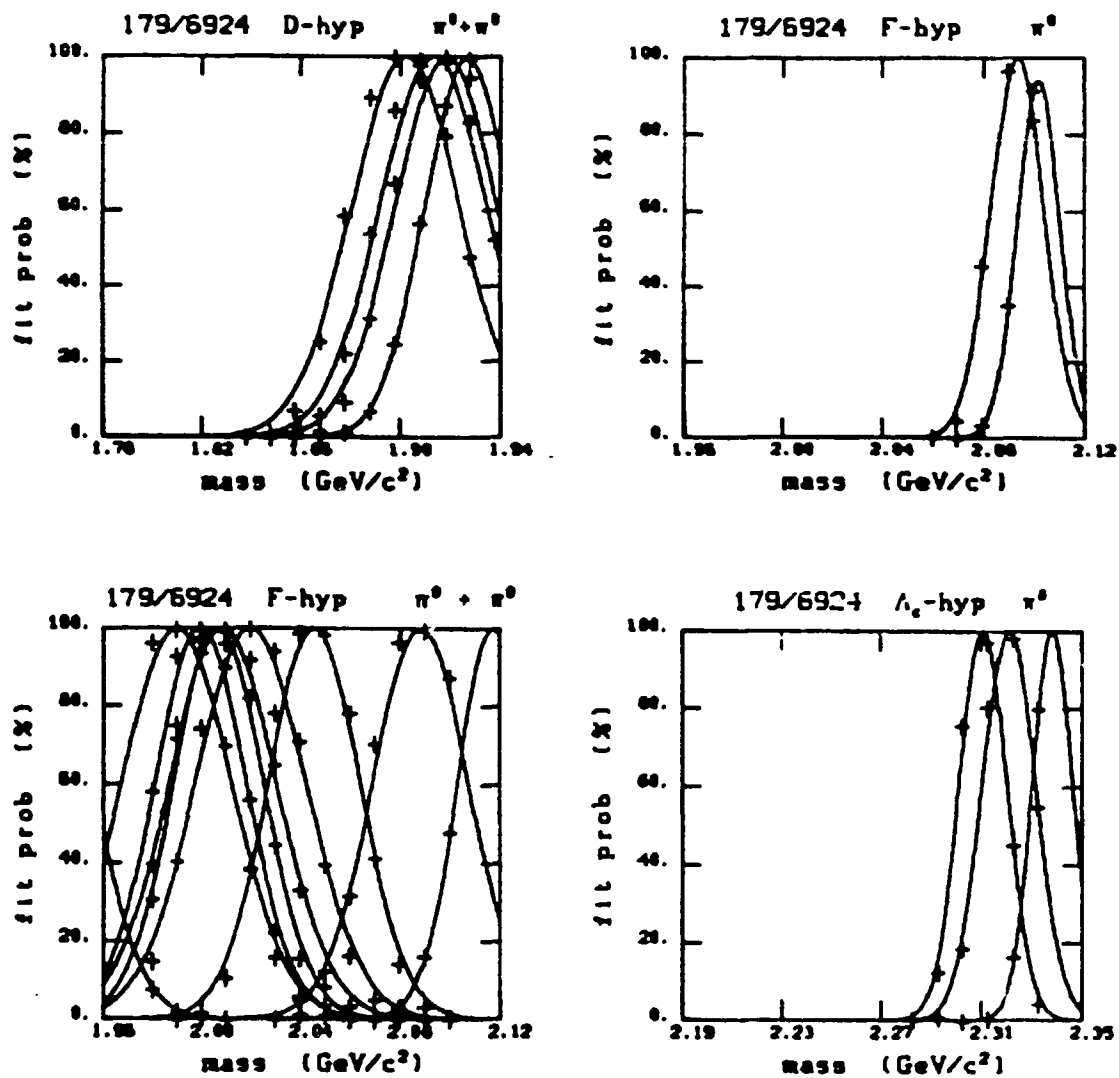


Fig. 24 (c-f). Continued.

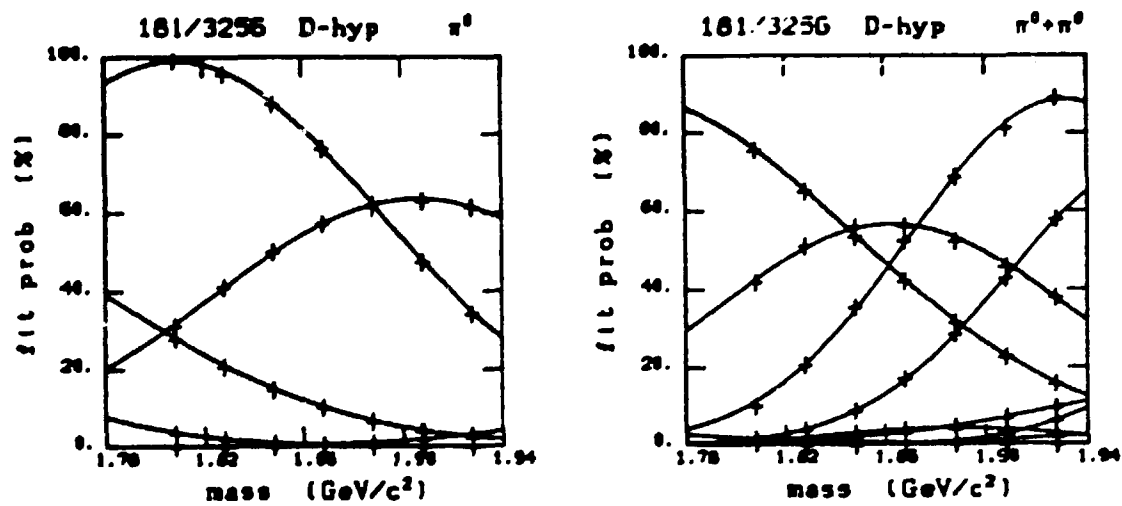


Fig. 25 (a-b). Fit probability vs. mass, frame 181-3256. (Continued.)

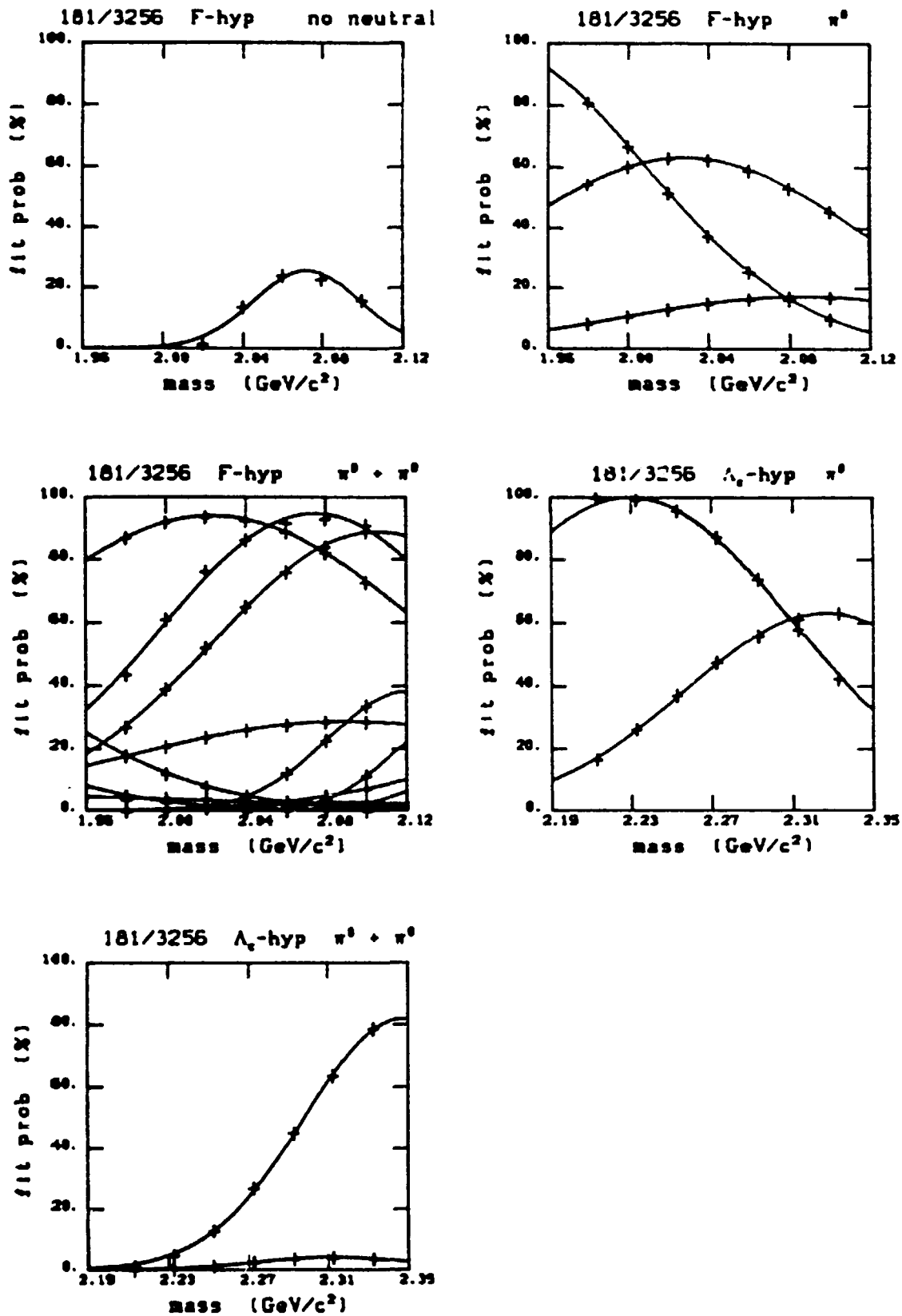


Fig. 25 (c-g). Continued.

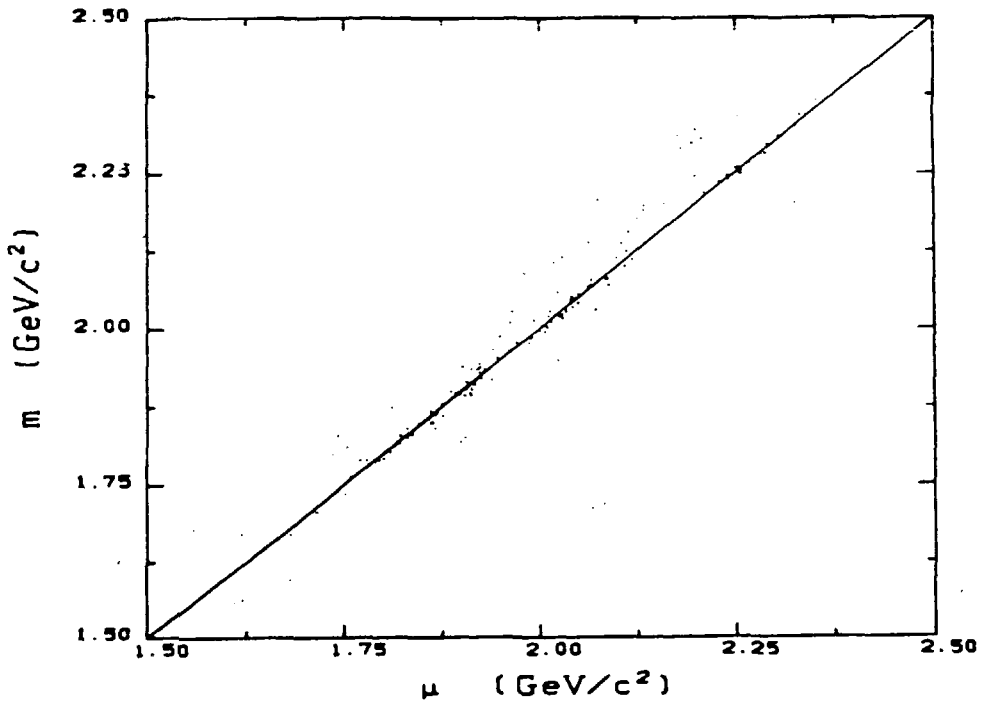
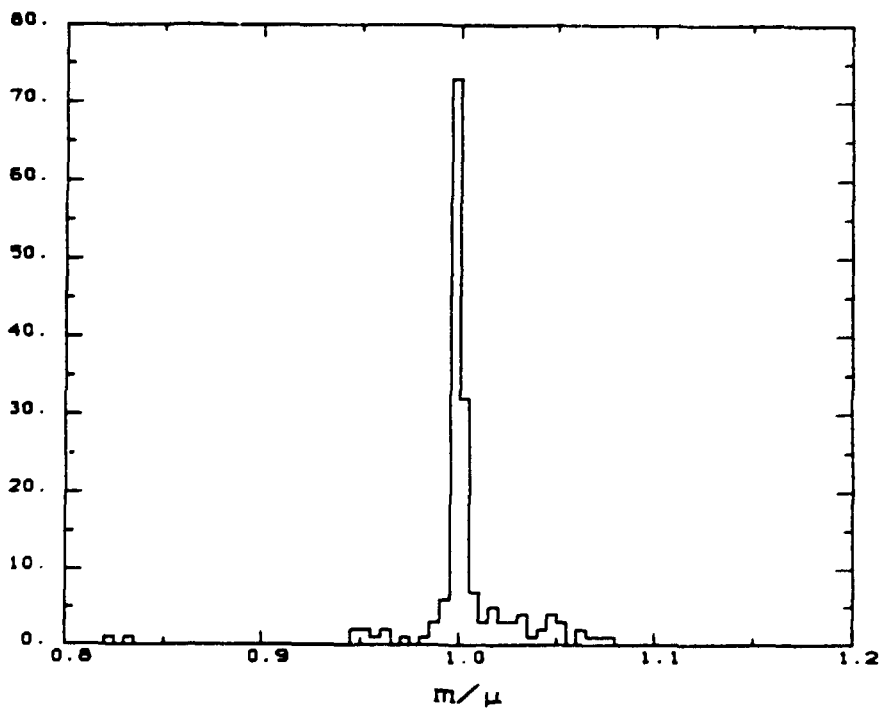


Fig. 26 a) Invariant mass m calculated from measured variables plotted versus the mean value of the fitted gaussian ($=\mu$) for 165 hypotheses. The solid line represents $m = \mu$.



b) The ratio m/μ .

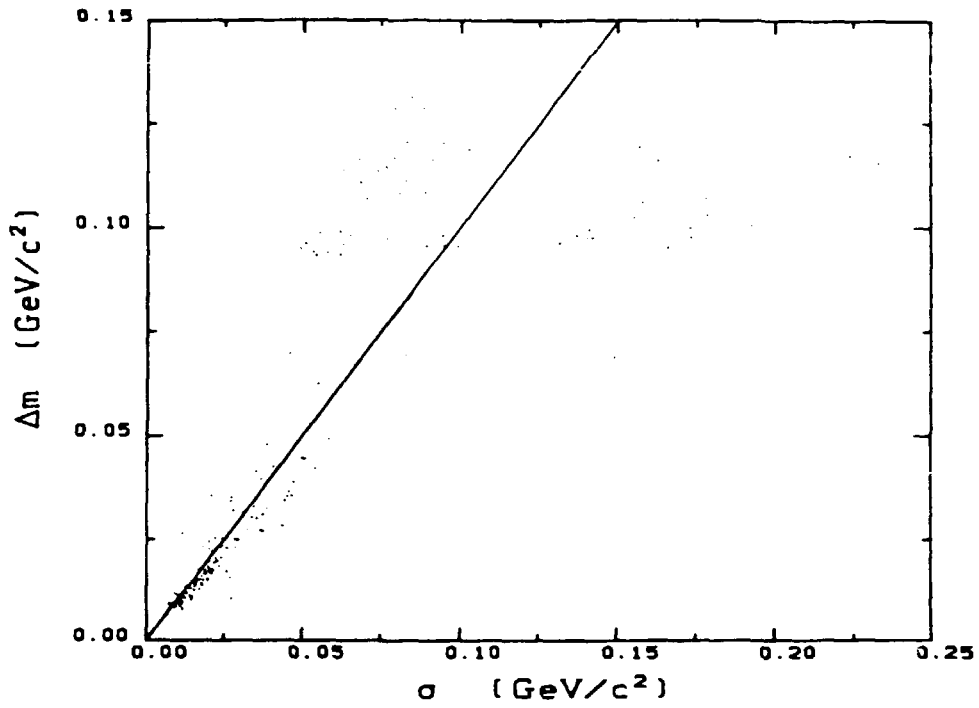
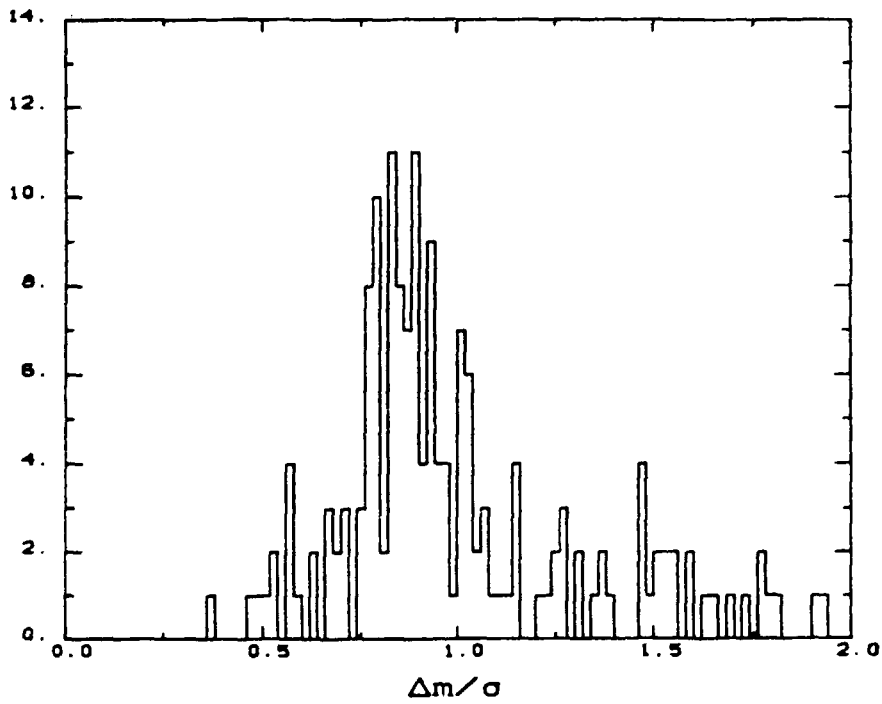


Fig. 27 a) Error in invariant mass plotted versus the width ($=\sigma$) of the fitted gaussian. The solid line represents $\Delta m = \sigma$.



b) The ratio $\Delta m / \sigma$.

Table 1. Comparison of the result of the choices of hypotheses using criteria I and II (probability plots).

Roll-frame	Criteria I	Criteria II
069-3364	$D^- \rightarrow K^+ \pi^- \pi^-$	$D^- \rightarrow K^+ \pi^- \pi^-$
072-5635	$D^- \rightarrow K^+ \pi^- \pi^- \pi^0$	$D^- \rightarrow K^+ \pi^- \pi^- \pi^0$
075-7361	$F^+ \rightarrow \eta \pi^+ \pi^0$	$F^+ \rightarrow \eta \pi^+ \pi^0$
081-0380	$F^- \rightarrow \pi^+ \pi^- \pi^- \pi^0$	$F^- \rightarrow \pi^+ \pi^- \pi^- \pi^0$
085-1753	$D^- \rightarrow K^+ \pi^- \pi^-$	$F^- \rightarrow K^+ K^- \pi^-$
087-6800	$D^- \rightarrow K^+ \pi^- \pi^- \pi^0$	D^-/F^- amb.
102-4843	$D^- \rightarrow K^+ \pi^- \pi^-$	$D^- \rightarrow K^+ \pi^- \pi^-$
103-7889	$D^- \rightarrow K^+ \pi^- \pi^-$	$D^- \rightarrow K^+ \pi^- \pi^-$
113-8206	$D^- \rightarrow K^+ \pi^- \pi^-$	$D^- \rightarrow K^+ \pi^- \pi^-$
116-1135	$D^+ \rightarrow K^- \pi^+ \pi^+ \pi^0$	D^+/F^+ amb.
120-6828	F^+/Λ_c amb.	F^+/Λ_c amb.
144-5401	$D^+ \rightarrow K^- \pi^+ \pi^+ \pi^0$	$D^+/F^+/\Lambda_c$ amb.
149-1190	$D^+/F^+/\Lambda_c$ amb.	$D^+/F^+/\Lambda_c$ amb.
149-2024	$D^- \rightarrow K^+ \pi^- \pi^-$	$D^- \rightarrow K^+ \pi^- \pi^-$
152-6910	$D^- \rightarrow K^+ \pi^- \pi^-$	$D^- \rightarrow K^+ \pi^- \pi^-$
158-6037	$D^+/F^+/\Lambda_c$ amb.	$D^+/F^+/\Lambda_c$ amb.
162-8219	$F^- \rightarrow K^+ K^- \pi^- \pi^0$	$F^- \rightarrow K^+ K^- \pi^- \pi^0$
173-0217	D^+/F^+ amb.	D^+/F^+ amb.
178-0649	$D^+ \rightarrow K^- \pi^+ \pi^+$	D^+/Λ_c amb.
178-0653	$D^+ \rightarrow K^- \pi^+ \pi^+ \pi^0$	$D^+/F^+/\Lambda_c$ amb.
179-6924	$D^+ \rightarrow K^- \pi^+ \pi^+$	$D^+ \rightarrow K^- \pi^+ \pi^+$
181-3256	$D^+ \rightarrow K^- \pi^+ \pi^+ \pi^0$	$D^+ \rightarrow K^- \pi^+ \pi^+ \pi^0$

Table 2. Changes in the D-sample that would be obtained by using criteria II instead of criteria I.

Criteria II	Criteria I	
	D → Krrr	D → Krrrr ^o
D → Krrr	7	
→ Krrrr ^o		2
F	1	
D/F amb.		2
D/Λ _c amb.	1	
D/F/Λ _c amb.		2